PREPARATION AND CHARACTERIZATION OF DURIAN HUSK-BASED BIOCOMPOSITE FILMS REINFORCED WITH NANOCELLULOSE FROM PINEAPPLE LEAVES AND CORN HUSKS

NATTAPRON SIRIBANLUEHAN

A THESIS SUBMITTED IN PARTIAL FULFILLMENT OF
THE REQUIREMENTS FOR MASTER DEGREE OF ENGINEERING
IN CHEMICAL ENGINEERING
FACULTY OF ENGINEERING
BURAPHA UNIVERSITY
2024

การเตรียมและการศึกษาคุณลักษณะของฟิล์มคอมโพสิตชีวภาพจากเปลือกทุเรียนเสริมแรงด้วยนาโนเซลลูโลสจากใบสับปะรดและเปลือกข้าวโพด

ณัฐพร ศิริบรรลือหาญ

วิทยานิพนธ์นี้เป็นส่วนหนึ่งของการศึกษาตามหลักสูตรวิศวกรรมศาสตรมหาบัณฑิต
สาขาวิชาวิศวกรรมเคมี
คณะวิศวกรรมศาสตร์ มหาวิทยาลัยบูรพา
2567

PREPARATION AND CHARACTERIZATION OF DURIAN HUSK-BASED BIOCOMPOSITE FILMS REINFORCED WITH NANOCELLULOSE FROM PINEAPPLE LEAVES AND CORN HUSKS

NATTAPRON SIRIBANLUEHAN

A THESIS SUBMITTED IN PARTIAL FULFILLMENT OF
THE REQUIREMENTS FOR MASTER DEGREE OF ENGINEERING
IN CHEMICAL ENGINEERING
FACULTY OF ENGINEERING
BURAPHA UNIVERSITY
2024

The Thesis of Nattapron Siribanluehan has been approved by the examining committee to be partial fulfillment of the requirements for the Master Degree of Engineering in Chemical Engineering of Burapha University

Advisory Committee

Principal advisor

.....

(Associate Professor Piyachat Wattanachai)

Examining Committee

..... Principal examiner
(Associate Professor Sopark Sonwai)

..... Member
(Associate Professor Piyachat Wattanachai)

..... Member
(Associate Professor Soipatta Soisuwan)

..... Member
(Assistant Professor Settakorn Upasen)

..... Dean of the Faculty of Engineering
(Assistant Professor Nayot Kurukitkoson)

.....

This Thesis has been approved by Graduate School Burapha University to be partial fulfillment of the requirements for the Master Degree of Engineering in Chemical Engineering of Burapha University

..... Dean of Graduate School
(Associate Professor Dr. Witawat Jangiam)

.....

65910172: MAJOR: CHEMICAL ENGINEERING; M.Eng. (CHEMICAL ENGINEERING)
KEYWORDS: BIOCOMPOSITE FILM/ DURAIAN HUSKS/ CORN HUSK NANOCELLULOSE/ PINEAPPLE LEAVES NANOCELLULOSE/ MECHANICAL PROPERTIES

NATTAPRON SIRIBANLUEHAN : PREPARATION AND CHARACTERIZATION OF DURIAN HUSK-BASED BIOCOMPOSITE FILMS REINFORCED WITH NANOCELLULOSE FROM PINEAPPLE LEAVES AND CORN HUSKS. ADVISORY COMMITTEE: PIYACHAT WATTANACHAI, Ph.D. 2024.

Various agricultural wastes generally contain cellulose, which is one type of biopolymers and hence can be used to replace synthetic, non-biodegradable materials. In this study, corn husks nanocellulose (CHNc) and pineapple leaves nanocellulose (PLNc) were incorporated into carboxymethyl cellulose-based film made from durian husks (CMC_{DH}) with different nanocellulose contents (15, 30, and 45 wt%) through solvent-casting method as reinforcement. Durian husks cellulose (DHC) was obtained via alkaline and bleaching processes before CMC_{DH} synthesis by carboxymethylation using sodium hydroxide and sodium monochloroacetate in isopropyl alcohol. The corn husks (CH) and pineapple leaves (PL) were treated through alkaline and bleaching treatments before synthesizing nanocellulose using acid hydrolysis. The results from Fourier transform infrared spectroscopy (FTIR), transmission electron microscopy (TEM), and X-ray diffraction (XRD) indicated that alkaline and bleaching treatments effectively removed non-cellulosic components. Additionally, during the carboxylation reaction, the hydroxyl group on DHC was substituted with a carboxyl group. TEM images indicated the successful preparation of CHNc and PLNc which achieved rod-like in shape and nanoscale in size, with a length and diameter of approximately 206.45 ± 41.10 nm × 7.24 ± 1.38 nm, and 150.68 ± 42.10 nm × 6.52 ± 0.96 nm, respectively. XRD data showed the increased crystallinity index (CI) values of CHNc and PLNc to 63.94 and 62.27%, respectively, as compared to those the untreated CH and PL at 32.76 and 46.01%, respectively, implying the effective removal of lignin and hemicellulose. The CMC_{DH} composite films were examined for their UV-visible light transmittance,

water vapor transmission rates (WVTR), mechanical properties, thermal stability, and biodegradability. The CMC_{DH} composite films prepared in this work has yellowish appearance compared to commercial CMC composite films (CMC_{com}). The addition of nanocellulose (CHNc and PLNc) reduced the UV-visible light transparency of the CMC_{DH} films but improved their water barrier, thermal stability, and tensile strength. The WVTR decreased from 2.77 to 2.33 and 2.10 gm^2/h with 30 wt% of CHNc and PLNc, respectively. The highest tensile strength was obtained from CMC_{DH}/PLNc(30%) with a value of 5.06 ± 0.83 MPa. However, agglomeration of PLNc at 45 wt% resulting in a decrease in tensile strength to 3.78 ± 0.44 MPa. Scanning electron microscopy (SEM) also confirmed the agglomeration of PLNc at high PLNc concentration. According to Thermogravimetric Analysis (TGA) and Differential Scanning Calorimeter (DSC), the addition of nanocellulose delayed decomposition temperature of CMC_{DH} composite films by approximately 10 °C. Photodegradation study of the film under UV light irradiation of the wavelength of 320-400 nm indicated that after 2 days of irradiation, all the films were hard and brittle. However, the films' color did not alter after 7 days of irradiation. For biodegradation investigation via soil burial test, all of the composite films completely degraded within 3 days. Therefore, the CMC_{DH} biocomposite films prepared in this research can be an alternative material for solving environmental issues and promoting sustainable materials in packaging applications. In addition, this research counteracts with Bio-Circular-Green (BCG) economy model of Thailand.

ACKNOWLEDGEMENTS

This research work could not have been accomplished without the assistance and support of all these individuals and organizations. First of all, I would like to thank my advisor, Assoc. Prof. Piyachat Wattanachai, for the valuable guidance, encouragement, suggestions, and all the helpful support. I am grateful for the scholarship provided by (i) Department of Chemical Engineering, Faculty of Engineering, Burapha University (BUU) (The 2nd of the project to promote and enhance the quality of graduate studies for developing sustainable research assistants, 2/2565), (ii) Thailand Science Research and Innovation (TSRI), and (iii) the National Science Research and Innovation Fund (NSRF) (Fundamental Fund : Grant no.32/2566 and 87/2567). Lastly, I am deeply grateful to my family for their invaluable support and encouragement.

Nattapron Siribanluehan

TABLE OF CONTENTS

Page

LIST OF TABLES

Page

LIST OF FIGURES

Page

CHAPTER 1
INTRODUCTION

Statements and significance of the problems

Flexible packaging demand has risen dramatically in recent years due to food consumption growth. Synthetic polymers derived from petroleum are the most convenient and cost-effective packaging materials (Ncube et al., 2020). However, these polymers cannot decompose, and hence they generate large amounts of plastic wastes (Ng et al., 2017). Furthermore, due to an increase in fuel demand used for energy production for both households and industries, the cost of petroleum has risen significantly. Despite widespread uses of petroleum-based plastics, fossil fuels soon will not satisfy future needs. The development of biocomposite films based on carboxymethyl cellulose (CMC) has significant promise for solving current environmental issues caused by traditional plastics and promoting sustainable materials. Until now, many researchers have reported on the extraction of CMC from a wide range of natural source materials, particularly agricultural wastes, such as durian rind (Rachtanapun et al., 2012; Upasen et al., 2023), and corn cob (Jia et al., 2016). Recently, cellulose extraction from agricultural residues has become a popular topic of research. In Thailand, durian is an iconic fruit. Durian husks are typically thrown away as waste, resulting damaging impacts to the environment. In this research, durian husks were selected as a main material and natural source of cellulose to produce biocomposite films. Due to its non-toxicity, affordability, and biodegradability, CMC has drawn a lot of interest as an edible and recyclable film material for food packaging. However, CMC film's poor mechanical and water vapor barrier properties limit its potential application in the food packaging industry (de Melo Fiori et al., 2019).

Nanocellulose, an alternative nanomaterial derived from natural cellulosic fibers, is a potential sustainable reinforcement for biopolymers. Any agricultural biomass that contains cellulose, such as pineapple leaves (Fitriani Fitriani, Sri Aprilia, Nasrul Arahman, Muhammad R. Bilad, Amri Amin, et al., 2021), corn husks (Yang et al., 2017) and other natural fibers, can be used to prepare nanocellulose. High

crystallinity, high thermal stability, hydrophilic nature, biodegradability, and renewability are the main reasons that nanocellulose is utilized as reinforcing material in biocomposite films to improve the mechanical and barrier properties of biocomposite film (Sharma et al., 2018). This research was hence aimed to investigate the effect of nanocellulose derived from different agricultural wastes (pineapple leaves and corn husks) and amount of nanocellulose on the reinforcement of durian husks-based biocomposite films.

Objectives

1. To study the effect of nanocellulose derived from different agricultural wastes (pineapple leaves and corn husks) on properties of durian husks-based biocomposite films.
2. To investigate the effect of the amount of nanocellulose reinforcement on the properties of durian husks-based biocomposite films.

Scope of the study

1. Synthesis of carboxymethyl cellulose (CMC) from durian husks via carboxymethylation.
2. Synthesis of nanocellulose from pineapple leaves and corn husks via acid hydrolysis.
3. Preparation of biocomposite films from durian husks reinforced with nanocellulose from pineapple leaves and corn husks via solution casting method.
4. Study of the properties of the biocomposite films including FTIR, XRD, TEM, SEM, TGA, DSC, color measurement, mechanical properties, water vapor transmittance rate, photodegradability, and biodegradability.

Contribution to knowledge

1. It is possible to produce biocomposite films from durian husks reinforced with nanocellulose derived from pineapple leaves and corn husks. These agricultural waste materials can be utilized as valuable resources for future applications.

2. This approach offers the potential to reduce the amount of agricultural and plastic waste generated. It serves as an alternative option for environmental friendly packaging plastics.

CHAPTER 2
REVIEW LITERAURES

Bioplastic

Bioplastic is a term used to describe plastic materials that are either biobased, biodegradable, or have both characteristics. While biodegradation is a chemical process by which a substance is transformed into water, carbon dioxide, and compost by the activity of naturally occurring microbes under normal environmental circumstances, the word "biobased" suggests that its components are mostly obtained from biomass. Bioplastics (both biodegradable and nonbiodegradable) are typically divided into four major categories: directly produced from biomass, synthesized from biobased monomers, from petrochemicals, and produced by microorganisms (Fig. 1). Nowadays, they're used as environmental friendly substitutes for many common plastics. They are a wide range of materials with different qualities and uses. Many traditional plastics can now be replaced with more environmental friendly materials (Ortega et al., 2021).

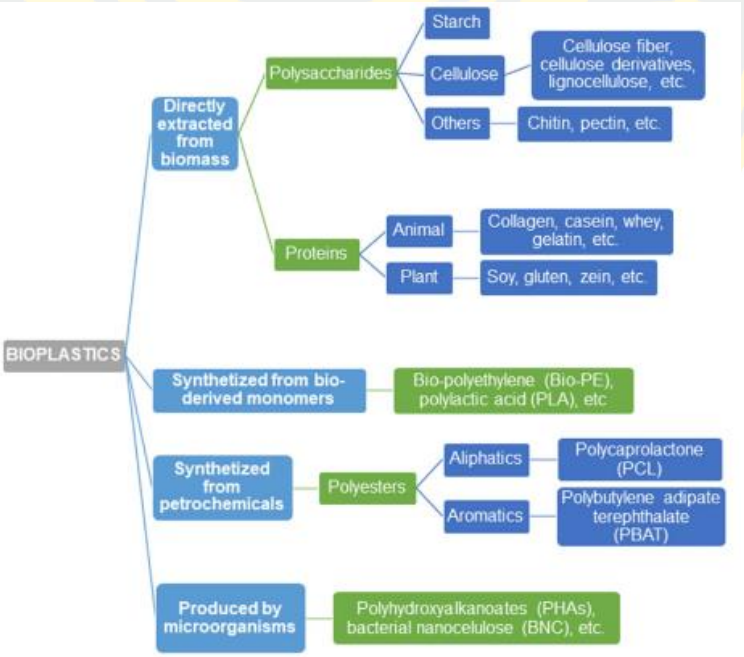

Figure 1 Bioplastics classification according to production process and origin with some examples.
(Ortega et al., 2021)

The most frequent macromolecules in nature are polysaccharides, and many of them may be used as feedstock for bioplastics. Plants, microbes, phytoplankton, and mammals produce polysaccharides, making them non-toxic and abundant. Due to their physicochemical qualities, many of them may be modified chemically and physically to improve their properties for use in a wide range of biomaterials (Mohammed et al., 2021). One commonly available polysaccharide is produced from renewable resources, particularly cellulose. A major source of cellulose is plants. Approximately 30 to 40% of cellulose is found in herbaceous plants, 45 to 50% in woods, 60 to 70% in bast plants (flax, jute, etc.), and up to 90% in cotton fibers. Plant-based materials frequently contain cellulose together with other substances, including lignin, pectin, and hemicellulose. Plant materials generally contain between 40 and 55% cellulose, 15 - 35% lignin, and 25 - 40% hemicellulose (Penjumras et al., 2014).

Lignocellulosic materials

Lignocellulosic materials mainly compose of cellulose, hemicellulose, and lignin, and hence they are one of the most significant natural sources of biopolymers and high-value materials. Many researchers focus on utilizing agricultural residues due to their high content of lignocellulosic matter, which are desirable due to their biodegradability, low density, and outstanding mechanical qualities (Collazo-Bigliardi et al., 2019).

Cellulose is a long-chain polysaccharide composed of repeating glucose molecules ($C_6H_{10}O_6$) as shown in Fig.2. Cellulose chains are oriented and have two ends: reducing ends containing free hydroxyl groups, and nonreducing ends containing o-glycosidic bonds (Ouarhim et al., 2019). As a structural component of plant cell walls, cellulose provides strength, rigidity, and support to plants. It is found in abundance in plant-derived materials, such as wood, cotton, hemp, jute, and various agricultural residues (Zhao et al., 2019). Carboxymethyl cellulose (CMC), which is cellulose derivative and obtained by substituting some hydroxyl groups on the cellulose chain with carboxymethyl groups ($-CH_2COOH$), are widely used recently This is because the modification imparts water solubility and improved film-forming properties to cellulose, expanding its range of applications.

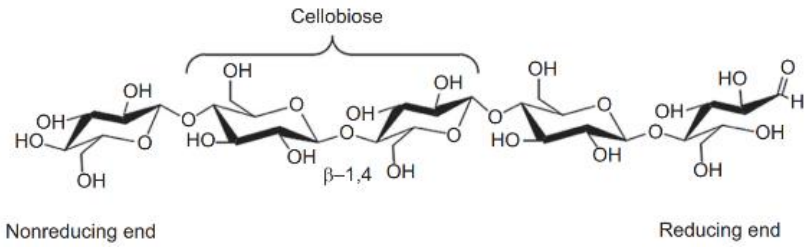

Figure 2 Cellulose chain structure.
(Bledzki & Jaszkiewicz, 2010)

Hemicellulose contains several sugars, including xylose ($C_5H_{10}O_5$), mannose ($C_6H_{12}O_6$), arabinose ($C_5H_{10}O_5$), glucose ($C_6H_{12}O_6$), and glucuronic acid ($C_6H_{10}O_7$) as shown in Fig. 3. In contrast to cellulose, hemicellulose has a lot of chain ramifications. Generally, it's noncrystalline and it differs between various plant species. (Ouarhim et al., 2019). It dissolves in alkaline solutions and hydrolyzes in acids (John & Anandjiwala, 2008).

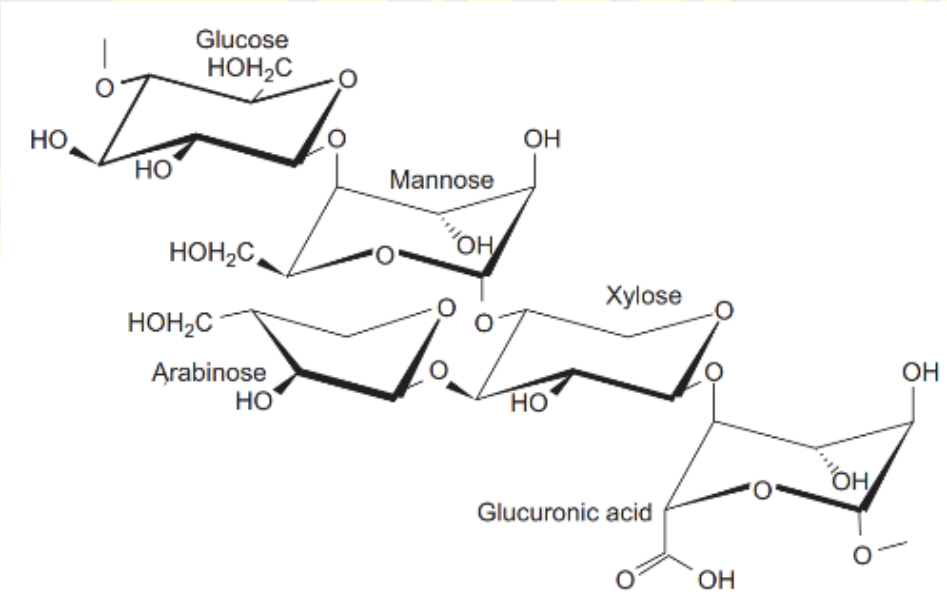

Figure 3 Hemicellulose structure.

Lignin is a three-dimensional phenolic polymer (Fig. 4). This element supports cell walls rigidity and protects plants from harmful organisms. It is completely amorphous and hydrophobic. Its mechanical qualities are less than

cellulose's (Reddy & Yang, 2005), and it makes natural fibers coarse and stiff (Dai et al., 2018b). Lignin is easily condensable with phenol and soluble in alkali, but cannot be hydrolyzed by acids (Ouarhim et al., 2019).

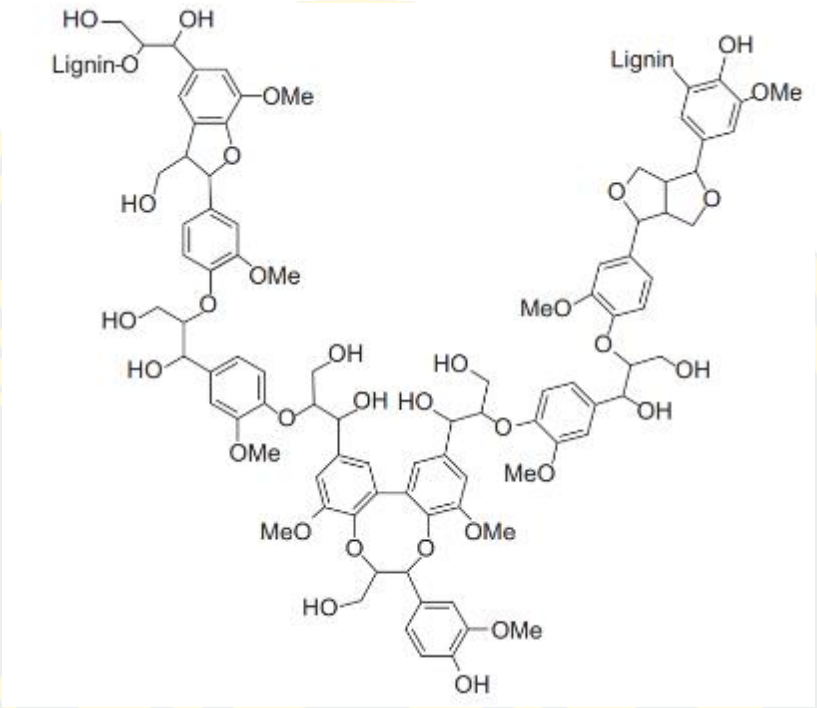

Figure 4 A lignin chain structure.
(Arrakhiz et al., 2012)

Chemical treatments

1. Alkaline treatment

Alkaline treatment affects natural fiber surfaces by removing lignin, hemicellulose, wax, and oils (Faruk et al., 2012). The eliminated lignin and hemicellulose result in the increasing adhesion of the matrix and fibers. According to reports, cellulose has the highest strength and rigidity components (Al-Khanbashi et al., 2005). The most frequent chemical used in alkaline treatment is sodium hydroxide (NaOH).

Chen et al. (2018) studied the wettability of individual bamboo fibers together with their thermal stability. NaOH solutions of various concentrations (6, 8, 10, 15, and 25%) were used to treat individual bamboo fibers. They found that

after treatment with NaOH, the surface roughness of fibers increased. The wettability of bamboo fibers was improved after treated with low concentrations of NaOH but deteriorated with high concentrations of NaOH (25%). Thermal analysis showed that after treatment with NaOH at low concentrations (6, 8, and 10%), the beginning and peak of decomposition were shifted to higher temperatures, indicating an improvement in the thermal stability of fibers because of the removal of hemicellulose. However, after treatment at higher concentrations (15 and 25%), the thermal stability was compromised.

Furthermore, the effect of NaOH concentration (0, 5, 10, 15, and 20 %w/v) on the properties of tapioca solid waste (TSW) was investigated by Arnata et al. (2022). The results revealed that alkaline treatment influenced changes in the chemical, physical, and thermal properties of cellulose derived from TSW. The amount of water and cellulose increased as the concentration of NaOH increased, whereas the amounts of starch, hemicellulose, and lignin decreased. At 10% NaOH concentration, the fiber dimensions increased, and the surface morphology becomes rougher, whereas at higher concentrations, the dimensions decreased. The degree of crystallinity and crystal size increased until the NaOH concentration reached 10%, but at higher concentrations, they tended to decrease (Arnata et al., 2022).

2. Bleaching treatment

After alkaline treatment, bleaching process is generally followed in order to eliminate the remaining lignin, and hence improve the surface adhesion between the matrix and fiber. Typically, the chemicals used in bleaching treatment including hydrogen peroxide (H_2O_2), sodium chlorite ($NaClO_2$), or sodium hypochlorite (NaClO) (Ouarhim et al., 2019). According to reports, bleaching with H_2O_2 demands multiple repetitions because lignin is not eliminated at the initial step, whereas bleaching with $NaClO_2$ only needs to be performed three times (Meriem et al., 2016). Washing is typically done after each bleaching. The presence of white fibers indicates that lignin is removed by oxidation processes, which implies an increase in surface area and matrix-fiber adhesion (Ouarhim et al., 2019).

Arnata et al. (2019) studied the effect of processing times by 30%w/v H_2O_2 (1 and 2 hours) on cellulose production. The results showed that the processing times had slightly effect on lignin removal. The highest yield of 31.32% was obtained from

1 hour and an increase of the processing time to 2 hours led to a slightly decrease in cellulose yield to 30.90%. On the other hand, the processing times are able to decrease the lignin contents of 8.85% (1 h) to 3.84% (2 h).

The synthesis of CMC

CMC is a water-soluble derivative of cellulose, which is the most abundant biopolymer found in nature. It is obtained through the chemical modification of cellulose, specifically the introduction of carboxymethyl groups (-CH_2COOH) onto the cellulose backbone (Fig. 5). This modification imparts water solubility and improved properties to cellulose, making CMC a versatile material for various applications. Due to its non-toxicity, affordability, and biodegradability, CMC has drawn a lot of interest as an edible and recyclable film material for food packaging (Kanikireddy et al., 2020). The introduction of natural fibers, such as jute, hemp, or kenaf, as reinforcement in CMC-based biocomposite films can significantly improve their mechanical and barrier properties (Zimniewska & Wladyka-Przybylak, 2016). In addition, blending nanoparticles such as nanoclay (Mohan & Kanny, 2015), nanocellouse (Oun & Rhim, 2015), and nanometal oxides (Fathi Achachlouei & Zahedi, 2018) into CMC matrix to create CMC-based composite film could be an effective way to enhance their thermal, mechanical, and barrier properties (Yunqing He, 2019). Among these, nanocellulose that has been derived from natural cellulosic resources has attracted a lot of attention because of its distinctive qualities, including renewability, biodegradability, biocompatibility, abundance, and light weight.

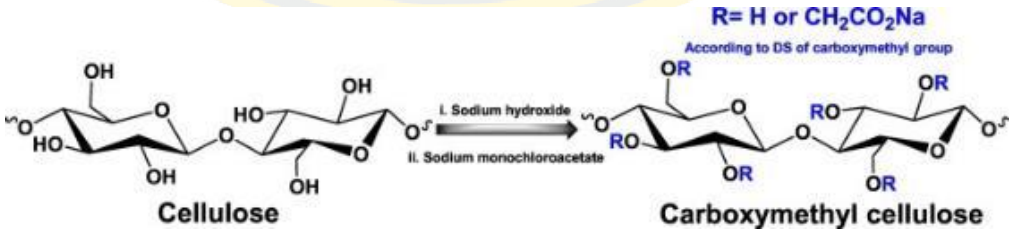

Figure 5 Carboxylation of cellulose
(Kanikireddy et al., 2020)

Until now, many researchers have reported on the extraction of CMC from a wide range of natural source materials, particularly agricultural wastes, such as durian

rind (Rachtanapun et al., 2012; Upasen et al., 2023), and corn cob (Jia et al., 2016). The synthesis of CMC from agricultural wastes as cellulose sources has been the subject of numerous studies. Togrul and Arslan (2003) investigated the rheological behavior of CMC extracted from sugar beet pulp cellulose and found that the degree of substitution (DS) value of CMC was 0.6670. The optimum carboxymethylation condition was at 3 g of sodium chloroacetate. Klunklin et al. (2021) carried out the synthesis of CMC from asparagus stalk end stalk (CMC_{as}) and investigated the impact of the NaOH concentrations from 20% to 60% on the mechanical characteristics of obtained CMC_{as} film. They found that 30% NaOH concentration provided the highest percent yield of CMC_{as} at 44.04% with the highest degree of substitution at 0.98. CMC_{as} films synthesized with 40% NaOH concentration exhibited the highest tensile strength of 44.59 MPa.

Rachtanapun et al. (2021) reported degree of substitution of CMC derived from nata de coco is depended on the monochloroacetic acid (MCA) concentration. It was found that CMC films synthesized using 24 g MCA with 15 g of cellulose produced the highest DS value at 0.83 and the highest tensile strength at 23.24 MPa.

Durian is a popular fruit in Thailand, Indonesia, and Malaysia, among other Southeast Asian nations. Thailand is the largest durian producer in Southeast Asia, growing as high as 1.1 million tons in 2020 (Economics, 2022). Only one-fourth to one-third of a durian fruit is edible and around 80% of the non-edible part is the rind (Masrol et al., 2015). The durian husk is typically thrown away and ends up in landfills or is burned, causing environmental problems.

Rachtanapun et al. (2012) produced CMC from durian rind using sodium monochloroacetate at different NaOH concentrations in the range of 20 to 60 g/100 mL. FTIR was used to investigate the chemical composition of the cellulose. The results showed that 30%w/v of NaOH produced the highest degree of substitution at 0.87 and the maximum viscosity, and hence it was considered to be the best conditions for carboxymethylation. They reported a reduction of crystallinity of CMC compared to extracted cellulose due to the breaking of hydrogen bonds from NaOH. In comparison to cellulose without alkalized with NaOH, the substitution of monochloroacetic acid molecules into cellulose polymers becomes easier because of the increased distance between cellulose molecules. This result agrees with the

cavendish banana cellulose crystallinity of CMC results, which decreased when alkalizing with 15 g/100 (Adinugraha et al., 2005). The highest tensile strength of 140.77 MPa and the highest water vapor transmission rate of 220.85 g/day. were also obtained from the CMC film prepared with 30%w/v NaOH. However, NaOH concentrations did not show an effect on percent elongation at break of the CMC films. Putri and Kurniyati (2016) investigated the effect of sodium chloroacetate towards the synthesis of CMC from durian peel. This study aimed to determine the yield of cellulose from durian peel with NaOH solution and sodium chloroacetate variations in the isolation process. They found that NaOH with a ratio of durian peel and NaOH 10% (w / v) at 1:15 gave the highest yield of cellulose of 64.72%. 7 g of sodium chloroacetate used during CMC synthesis resulted in the highest degree of substitution of CMC of 1.632.

Biocomposite films reinforced with Nanocellulose

A biocomposite film is a particular kind of material that consists of at least two components, including a polymer matrix and a biologically generated reinforcing agent. To produce a material with improved qualities, it combines the benefits of the matrix with the reinforcing ingredient.

Due to its unique properties, cellulose has recently gained attention as a promising nanocomposite. The main attributes of celluloses are low density, biocompatibility, biodegradability, environmental friendliness, affordability, and low energy consumption. They also have desirable mechanical qualities because of their high specific strength and modulus values. In polymer composites, celluloses are consequently utilized as reinforcing fillers. Several investigations on the extraction of nanocelluloses (NCs) from various raw materials, such as pineapple leaves (Santos et al., 2013; Upasen et al., 2023), and corn husk (Mendes et al., 2015), have been successful. Since nanotechnology has grown, science and business have focused on isolating NCs from biomass. Until now, there have been two primary methods for extracting NCs from biomass, i.e. mechanical methods, such as high-speed mixing (Uetani & Yano, 2011), and chemical methods, such as 2,2,6,6-tetramethylpiperidine-1-oxylradical (TEMPO)-oxidation (Liu et al., 2021) and acid hydrolysis (Yang et al., 2017). The isolation techniques have an impact on the NC's shape, size, and

characteristics. Cellulose nanofibril (CNF), which is NC obtained mechanically, has both amorphous and crystalline areas whereas cellulose nanocrystals (CNCs) are isolated from cellulose fibers using acid hydrolysis as the principal chemical method (Beck-Candanedo et al., 2005).

1. Nanocellulose from pineapple leaves

After pineapples are harvested, these leaves are often discarded. However, they may be a useful source of nanocellulose, a very strong and rigid type of cellulose that is found at the nanoscale. The mechanical, biodegradable, and barrier characteristics of the biocomposite film matrix may all be enhanced by adding nanocellulose derived from pineapple leaves. Usage of discarded pineapple leaves supports the circular economy strategy and environmental friendly packaging (Chawalitsakunchai et al., 2021).

Acid hydrolysis is a common and efficient method for hydrolyzing and removing most amorphous portions of celluloses. This is accomplished by treating the cellulose with a strong acid. Sulfuric acid is frequently used in the hydrolysis process. Nanocrystalline celluloses (NCCs) and cellulose nanocrystals (CNCs) are all names for hydrolyzed celluloses. NCCs must have at least one dimension with a length or diameter measured in nanometers (Nechyporchuk et al., 2016). NCC typically has lengths of 100–500 nm and diameters of 5–30 nm. It is a crystallized powder that is tasteless, odorless, and light in color (Xing et al., 2018). NCC possesses desirable qualities including a high capacity for reinforcing, strong thermal stability, biodegradability, and biocompatibility (Khan et al., 2021). The sources of the raw materials and process conditions, such as pretreatment technique, type and concentration of acid used, hydrolysis time, and hydrolysis temperature, are primary factors determining the structural characteristics of material (Pirich et al., 2019). Commercial NCC now offers a wide range of physicochemical, morphological, and thermal characteristics, leading to a wide range of applications. Additionally, they are frequently employed as reinforcing fillers in the biocomposite materials.

Fitriani et al. (2021) carried out sulfuric acid hydrolysis of pineapple crown leaf (PCL) to obtain NCC and investigated how the hydrolysis time (1-3 hours) affected the characteristics of NCC. The results showed that NCC has a high crystalline and a rod-like particle structure. The maximum NCC yield of 79.37% was

attained after an hour of hydrolysis. Furthermore, the NCC sizes decreased with increasing hydrolysis time. The decrease in the crystallite size of NCC could be attributed to the process of acid break down the glycosidic bonds in NCC into the smaller sizes. Chawalitsakunchai et al. (2021) synthesized the nanocellulose (CNCs) from pineapple leaves. They were in rod-like morphology with diameters and lengths of the CNCs of 3-5 nm and 100–150 nm, respectively. The CNCs were blended into natural rubber (NR) composites as a reinforcing agent. The results indicated that, due to a homogenous distribution of CNCs in the composites, the addition of CNCs at an amount of 2.5 phr enhanced the tensile strength of NR composites (19.4 MPa).

Fitriani et al. (2021) examined how pineapple crown leaf (PCL) NCC loadings in the range of 0% to 10% w/w affected whey protein isolate (WPI) films. The films' mechanical, physical, chemical, and thermal properties were examined. The film thickness increased as the NCC content increased. As the NCC loadings increased, the film transparency, moisture content and absorption continuously reduced. On the other hand, thermal stability of the films was increased with an increase in NCC loading. The composite film with 7% NCC loading possessed the highest the tensile strength at 5.1 MPa.

2. Nanocellulose from corn husks

Several researchers around the world have been developing techniques to extract NC from corn husks in recent years. Poly (vinyl alcohol) films reinforcing nanocellulose extracted from maize husk using high intensity ultrasonication were produced and their characteristics were investigated by Xiao et al. (2016) . The obtained nanofibrillated cellulose (NFC) had an average diameter of 146.60 and length of tens microns. They prepared PVA films containing different nanofibrillated cellulose (NFC) concentrations at 0.5%, 1%, 3%, 5%, 7%, and 9% w/w. It was found that tensile strength of PVA/1%-NFC film was increased by 1.47 time compared to that of pure PVA film. Moreover, the PVA/1%-NFC film had a high visible light transmittance of 80%. Yang et al. (2017) synthesized the nanocellulose (NC) from corn husk via acid hydrolysis. The average diameters and lengths of the corn husk NC were 26.9 ± 3.35 nm and 162 ± 35.9 nm, respectively. Moreover, the corn husk NC extracted by acid hydrolysis exhibited highly crystallinity and thermal stability with a low aspect ratio. NC can be obtained from maize husk using a variety of methods, but

none of this research investigated its dispersion stability, an important NC property. No research has evaluated the structure and properties of NC after acid hydrolysis, TEMPO oxidation, and high intensity ultrasonication. The study of how different extraction techniques affect NC will help us use corn husk NC more effectively. Hence, the objectives of this study were to investigate the effect of nanocellulose reinforcement (pineapple leaves and corn husks) and amount of reinforcement on the properties of durian husks-based biocomposite films.

CHAPTER 3
RESEARCH METHODS

Materials

1. Mon Thong durian rinds from Rayong, Thailand, was collected from a durian seller in Chonburi.
2. Pineapple leaves were obtained from Khun Wira Pineapple farm in Sriracha, Chonburi.
3. Corn husks were obtained from a corn seller in Phra Nakhon Sri Ayutthaya.
4. 98% purity sodium hydroxide (NaOH) was purchased from KEMAUS, Australia.
5. 30%w/v hydrogen peroxide (H_2O_2) was purchased from Chem-Supply Pty, Australia.
6. 99% purity isopropanol ($(CH_3)_2CHOH$) was obtained from KEMAUS, Australia.
7. 99.7% glacial acetic acid (CH_3COOH) was purchased from RCI Labscan, Thailand.
8. Monochloroacetic acid ($C_2H_3ClO_2$) was supplied by Merck, Germany.
9. 99.5% glycerol ($C_3H_8O_3$) was obtained from KEMAUS, Australia.
10. 99.8% ethanol (C_2H_5OH) was purchased from Liquor Distillery Organization, Thailand.
11. 98% sulfuric acid (H_2SO_4) was purchased from Anhui Fulltime Specialized Solvent & Reagents, China.
12. Deionized water

Equipment

1. Plastic grinder (Narongchai Engineering Company Limited, NAC 5)
2. Food blender (Hafele ECOM-294)
3. Hotplate magnetic stirrer (IKA, C-MAG HS 7)
4. A cheesecloth

5. Electrical furnace (France Etuves, XB058)
6. Sieves (100 and 300 µm)
7. Aluminium foil
8. Centrifuge Machine, Force 12 (Galaxy), Maximum Speed: 8,000 rpm
9. pH meter (Mettler Toledo FiveEasy ATC)
10. Bath sonicator (Labline GT SONIC-D3)
11. Petri dish
12. Dialysis membrane (14 kDa molecular weight cut-off) was ordered from Sigma-Aldrich.

Preparation of Durian Rind Cellulose

The durian rind cellulose preparation method was adopted from Khemkew and Kaewpirom (2016). Durind rinds were cleaned with water to remove dirt, sundried and chopped into small pieces. After that, the dried rinds were ground into powder using a plastic grinder. The alkaline treatment of durian rinds was performed using 10%w/v NaOH at ratio of 1:10 g/mL at 100 °C for 3 h and stirred using a magnetic stirrer bar. Aluminum foil was used to cover the beaker to prevent solvent evaporation. After the process was complete, the suspension was filtered using a cheesecloth and the cellulose fibers were washed several times by deionized water until the pH value of 7 was attained. Finally, the solid was dried at 60 °C for 3 h in an oven. The treated residue (1 g) was mixed with 30%w/v H_2O_2 (15 mL) at 70 °C for 3 h and stirred using a magnetic stirrer bar. Then, the suspension was filtered using a cheesecloth and washed until reaching a neutral pH. The bleached solid was dried at 60 °C for 3 h in an oven, followed by grinding using by a food processor and sieving into the sizes below 300 µm. Finally, the yield of cellulose (Y_C%) was calculated using the weight of extracted cellulose (W_C) and the weight of dried durian rinds (W_D) as shown in Eq. 1.

$$\text{Yc}\ (\%) = \frac{W_C}{W_D} \times 100 \qquad (1)$$

Synthesis of Carboxymethyl Cellulose (CMC)

The synthesis of CMC from durian rind was adopted from Rachtanapun et al. (2012). 3 g of cellulose was added into a mixed solution containing 10 mL of 30%w/v NaOH and 90 mL of isopropanol, and left at room temperature for 30 min. Then, 3.6 g of monochloroacetic acid was added into the mixture and was stirred for 2 h at ambient temperature using a magnetic stirrer bar. Next, aluminum foil was used to cover a beaker to prevent solvent evaporation, and then left standing in oven at 60 °C for 3 h. The mixture was separated into two phases: the liquid phase on the top layer and the solid phase at the bottom. The liquid phase was discarded while the solid was suspended in 20 mL of 70%v/v ethanol and neutralized using glacial acetic acid. The suspension was filtered using filter paper, and then the solid was again suspended in 60 mL of 70%v/v ethanol and left at room temperature for 10 min. Finally, the suspension was filtered and again washed with 60 mL of 70%v/v ethanol and dried in oven at 60 °C overnight. According to Eq. 2, the yield of CMC (Y_{CMC}%) was determined using the weights of cellulose (W_C) and CMC (W_{CMC}).

$$Y_{CMC}\ (\%) = \frac{W_{CMC}}{W_C} \times 100 \qquad (2)$$

Preparation of Pineapple Leaves and Corn Husk Cellulose

The preparation of pineapple leaf (PL) and corn husk (CH) cellulose was adopted by Chawalitsakunchai et al. (2021) and Dai et al. (2018). Firstly, PL/CH were cleaned with water to remove dirt, chopped into approximately 2 cm × 5 cm, dried, and ground using a food blender. Alkaline treatment of the fibers was performed using 5%w/v NaOH at a ratio of 1:10 g/mL and 100 °C for 3 h. After the process was complete, the suspension was filtered using a cheesecloth and the cellulose fibers were washed several times by deionized water until the pH value of 7 was attained. Then, the solid was dried at 60 °C for 3 h. Then, the solid was dried at 60°C for 3 h. The treated residue (1 g) was added with 7.5%w/v $NaClO_2$ solution at a ratio of 1:20 g/mL (adjust pH 3.8-4.0 by 4 mol/L of glacial acetic acid) at 70 °C for 3 h and stirred using a magnetic stirrer bar. Then, the suspension was filtered using a cheesecloth and

washed until reaching a neutral pH. The bleached solid was dried at 60 °C for 3 h, followed by grinding using a food processor and sieving into sizes below 300 µm.

Isolation of Pineapple Leave and Corn Husk nanocellulose

Isolation of PL/CH was performed using acid hydrolysis method. The bleached cellulose (1 g) was digested with 10 mL of 64%w/w H_2SO_4 at 45 °C for 1 h and stirred using a magnetic stirrer bar. Next, the hydrolysis was stopped by adding tenfold cold distilled water, and the suspensions were centrifuged for 10 minutes at 8000 rpm to remove acids. The suspensions were dialyzed with dialysis membranes in deionized water for 7 days. Finally, the suspensions were sonicated for 30 minutes to obtain PL/CH nanocellulose (called as PLNc/CHNc in this thesis).

Biocomposite Films Preparation

The biocomposite films were prepared by the solution casting and evaporation method. 1.5 g of CMC was dissolved in 50 mL distilled water. The solution was stirred using a magnetic stirrer bar at 80 °C for 30 min. The suspension of PL or CH nanocellulose at loadings (15, 30 and 45%w/w of the weight of CMC) was slowly added while stirring in a magnetic stirrer bar for 1 h to form a homogeneous solution. The solution was left to cool down to room temperature, followed by addition of glycerol at a composition of 30%w/w of the weight of CMC (0.45 g). Then, the mixture was stirred for 30 min at room temperature and sonicated for 15 min. Finally, the solution was poured on a clean Petri dish (90 mm x 15 mm) and dried in an oven at 40 ◦C for 24 h. This procedure was modified from Dai et al., 2018.

Characterization

1. Degree of substitution (DS)

Degree of substitution (DS) of CMC refers to the average amount of hydroxyl groups in the cellulose structure replaced by carboxymethyl and sodium carboxymethyl groups at positions C2, 3, and 6. The DS was obtained using the standard method (ASTM D1961). 4 g of CMC was mixed with 75 ml of 95% (v/v) ethanol. Then, 5 ml of HNO_3 was added into the solution and stirred until boiling on

the heating plate. The mixture was agitated for a further 10 minutes at room temperature. The precipitate was filtered and rinsed with 95% (v/v) ethanol. Next, it was rinsed with pure methanol and subsequently dried in an oven at 105 °C for 3 h. 1 g of dried CMC was added into a mixed solution containing 100 mL of distilled water and 25 mL of 0.3M NaOH. The solution was stirred and heated to boiling for 15 minutes. Finally, approximately 2-3 drops of phenolphthalein indicator were dropped into the solution until a dark pink color was obtained and the solution was titrated with 0.3 M HCl. The DS was calculated based on Equations (3) and (4) (Mohamad Mazlan et al., 2022).

$$DS = \frac{0.162 \times A}{1-(0.058 \times A)} \quad (3)$$

$$A = \frac{(B \times C)-(D \times E)}{F} \quad (4)$$

Where:

A = milli-equivalents of consumed acid per gram of specimen

B = volume of NaOH (mL)

C = concentration of NaOH (M/L)

D = volume of consumed HCl (mL)

E = concentration of HCl (M/L)

F = the weights of CMC (g)

2. Transmission Electron Microscope (TEM)

The analysis was performed using a Philips TECNAI 20. The dilute nanocellulose suspension was dropped onto copper grids coated with a carbon support film. The characteristics and dimensions of the CNCs were presented in 2 dimensional images.

3. X-ray diffraction (XRD)

XRD patterns of the samples were obtained using an X-ray diffractometer (JEOL JDX-80-30). The scattering angle (2θ) was from 5 to 70° at a scanning speed of 2 °/min. The crystallinity index (CI) was calculated as given by Equations (5) (Nam et al., 2016).

$$CI\ (\%) = \frac{I_{200}-I_{am}}{I_{200}} \times 100 \quad (5)$$

where:

I_{200} = the maximum intensity of the (200) diffraction peak for cellulose Iβ at $2\theta = 22.5°$

I_{am} = the intensity of diffraction for amorphous part at $2\theta = 18.5°$

4. Fourier Transform Infrared Spectroscopy (FTIR)

Spectra analysis of the sample was performed using a PerkinElmer attenuated total reflectance-infrared spectroscopy (ATR-FTIR) spectrometer. Sixteen scans in the wavenumber range of 500 to 4000 cm^{-1} with the resolution of 4 cm^{-1} were conducted on each sample.

5. Thickness, Color values, and Transmittance

A Mitutoyo Digital Indicator Thickness Gauge with a resolution of 0.01 mm was used to measure the thickness of the film. To get average results, the measurement was conducted using three films of each mixture and five compositions. An Agilent Cary 60 Spectrophotometer was used to analyze the L*, a*, and b* values as well as the whiteness index (WI) and yellow index (YI) of the films. Three replicates of each film were tested. The spectrophotometer was also used to measure the light transmittance (%) of the films. The wavelength range of this dual-beam xenon flash spectrophotometer is 200 nm to 800 nm. sample.

6. Scanning Electron Microscope (SEM)

The biocomposite films were investigated using a field emission scanning electron microscope (FE-SEM). The analysis was performed using an LEO 1450 VP operated at an acceleration voltage of 15 kV. A Polaron Range Model SC 7620 Ion Sputter Coater was used for the gold sputtering of the samples.

7. Mechanical Properties

Tensile strength (TS), elongation at break (EB) and toughness of film specimens were measured using a Texture Analyzer, TA-XT plus, Stable Micro Systems Ltd., UK. Six to eight 1×10 cm^2 films were tested for each sample to obtain an average value and standard deviation. According to ASTM D882, the test was performed with a speed of 10 mm/min.

8. Thermogravimetric analysis (TGA)

Thermal characterization of the samples was performed using a thermogravimetric analyzer (Mettler Toledo TGA/DSC3+ module) with temperature range from 30 to 600 °C at a heating rate of 10 °C/min under N_2 atmosphere (20 mL/min). Derivative Thermogravimetry (DTG) curves were used to calculate the onset (T_{onset}) and maximum decomposition temperature (T_{max}) of samples, while TGA curves were used to determine the char residue at 600 °C (%).

9. Differential Scanning Calorimetry (DSC)

Differential Scanning Calorimetry (DSC) was used to determine the thermal transitions of the films where melting temperature (T_m) were analyzed using a Mettler Toledo DSC3 thermal analyzer. 3-5 mg of samples were placed onto a 40 μl aluminum crucible and covered with an aluminum lid. The tests were performed in the temperature range between 30 and 400°C at 10°C/min under a nitrogen atmosphere.

10. Water Vapor Transmission Rate (WVTR)

Water Vapor Transmission Rate (WVTR) test was performed via gravimetric method following ASTM E96. The film was used to cover a cup containing 5 g of silica gel and sealed with grease. The cup was placed in a desiccator containing water which is controlled to be at 28 °C and 90% relative humidity. The cup's weight was measured at 0 and 1 hour and WVTR was calculated according to Equation (6).

$$\text{WVTR } (g/m^2h) = \frac{W - W_0}{A \times T} \quad (6)$$

where:

W = weight of film specimen after 1 hour

W_0 = initial specimen weight

A = test area

T = time (hour) speed of 10 mm/min.

11. Photodegradation

The biocomposite films of the size of 1 x 5 cm^2 were exposed to UV irradiation in a photodegradation chamber as shown in Fig. 1. In the chamber (23 x 32 x 20 cm), the 50 watt UV lamp of the wavelength of 320-400 nm was placed 15 cm

from the surface of the films and irradiated continuously for 7 days. The physical appearance of the film was photographed every 24 hours to observe any changes. speed of 10 mm/min.

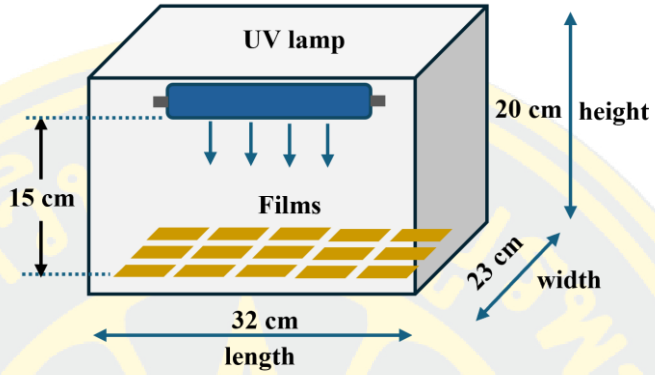

Figure 6 Schematic diagram of the photodegradation setup of biocomposite films.

12. Biodegradation

A biological degradation test was conducted via soil burial at a depth of 5 cm from the soil surface with a moisture content in the soil of approximately 80% at 25 ^{o}C for 3 days (Fig. 7). 3 pieces of 1x5 cm^2 film for each sample were placed on the soil and a plastic mesh was placed on top of the film before soil was added. The physical appearance of the film was photographed every 24 hours to observe any changes.

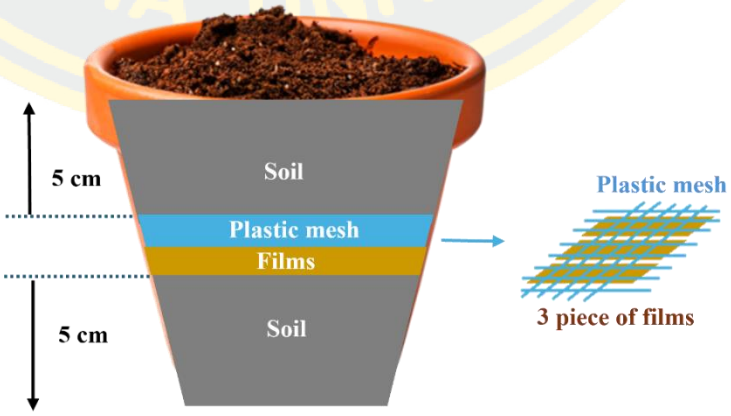

Figure 7 Schematic diagram of the biodegradation setup of biocomposite films.

CHAPTER 4
RESULTS

Yield of cellulose and CMC

In this research, the cellulose extraction was composed of two steps: namely, (1) alkaline treatment with NaOH, and (2) bleaching treatment with H_2O_2. The yield of extracted cellulose samples are shown in Table 1. Alkaline treatment with NaOH and delignification with H_2O_2 were performed to extract cellulose from durian rinds. The extraction yield of cellulose extracted from durian husks (DH) was 31.28 ± 0.78%, which is slightly lower than that obtained by Penjumras et al., (2014) (33.12%) but considerably higher than that achieved by Uppasen et al., (2023) (18.36%). Lubis et al. (2018) used Chesson-Datta technique to investigate the cellulose content in durian rinds and found the cellulose content of 57.4% while Charoenvai (2014) reported cellulose content of 42.7% characterized according to Technological Association of the Pulp and Paper Industry (TAPPI). In this research, similar processes were applied to extract cellulose from pineapple leaves (PL) and corn husks (CH) but $NaClO_2$ and CH_3COOH were used instead of H_2O_2 for bleaching step. Bleaching with $NaClO_2$ reduces the number of steps in the washing process. Moreover, bleaching with H_2O_2 demands multiple repetitions because lignin is not eliminated at the initial step, whereas bleaching with $NaClO_2$ only needs to be performed three times (Meriem et al., 2016). The yield of cellulose from pineapple leaves and corn husks was 16.97 ± 1.33% and 36.20 ± 1.20%, respectively. Similar yield of cellulose from pineapple leaves of 16.60 ± 1.42% was reported by Romruen et al. (2022). However, the yield of cellulose from corn husks from our findings (36.20 ± 1.20%) was considerably higher than that reported by Vallejo et al. (2021) (24.2 ± 0.7%) . Casanova et al. (2023) found that percent yield of obtained cellulose dependent on temperature and acid used for cellulose extraction. In addition, Sena Neto et al., (2015) and Leão et al., (2015) reported cellulose contents depend on plant species and soil and weather conditions for plantation. The cellulose from durian husks was modified by carboxymethylation reaction using monochloroacetic acid. The CMC yield from durian husks was 157.71 ± 3.98%, which is slightly higher than those obtained by Rachtanapun et al. 2012 (133-155%). Rachtanapun et al. 2012

found that as the concentration of sodium hydroxy increased from 20 to 30% w/v, CMC yield increased significantly from 120 to 165%. However, as the sodium hydroxy concentration increased more than 30% w/v, the CMC yields decreased. In addition to sodium hydroxy concentration, the chemical to cellulose ratio used in the carboxymethylation process also had a slight effect on CMC percent yield (Uppasen et al., 2023). The yield of CMC was higher than 100% because the molecular weight of the carboxymethyl group was higher than that of the hydroxyl group (Suhaimi et al., 2017).

Table 1 Yield of extracted cellulose and CMC.

Materials	Yield (%w/w)
Durian husks cellulose (DHC)	31.28 ± 0.78
Pineapple leaves cellulose (PLC)	16.97 ± 1.33
Corn husks cellulose (CHC)	36.20 ± 1.20
CMC-Durian husks (CMC_{DH})	157.71 ± 3.98

Degree of substitution

As can be seen from the structure of CMC (Figure 5 in Chapter 2), there are three hydroxyl groups in each glucose unit, namely C2, C3, and C6 hydroxyl groups. The degree of substitution (DS) is the average number of carboxymethyl groups replaced per monomer unit, with a range of 0 to 3. If all the three hydroxyl groups in each glucose unit are replaced by carboxymethyl, the DS can be defined as 3. If DS is lower than 0.4, the polymer is considered to be insoluble and only polymer swelling can be observed (Veeramachineni et al., 2016). In general, percent yield and DS of CMC are in the same trend, i.e. as the percent yield increases, DS also increases. The higher DS implies the higher solubility of that substance. In this work, the DS value of CMC_{DH} was 0.81 ± 0.04, which is only slightly lower than those obtained by Rachtanapun et al. 2012 (0.87). Kaewprachu et al. (2022) reported DS values of CMC extracted from pineapple leaf, bagasse, palm fruit husk, durian rind, and commercial CMC of 1.05, 0.78, 0.58, 0.87, and 0.7-0.8, respectively. Compared to CMC_{DH}, the

DS of commercial CMC (CMC_{com}), purchased from Hebei Yezhiyuan New Materials Co., Ltd., was lower (0.66 ± 0.04).

Transmission Electron Microscope (TEM)

The morphology of CHNc and PLNc were examined using TEM and are illustrated in Fig. 8. The results showed that the shape of CHNc was described as rod-like (Figure 8a-b), with an average length and diameter of the CHNc were 206.45 ± 41.10 nm and 7.24 ± 1.38 nm respectively which agrees quite well with data published by Chen et al. (2018), Kampeerapappun et al. (2015), and Yang et al. (2017), who reported that the nanocellulose extracted from corn husks had a diameter of 5-25 nm and a length of 150-250 nm. Similarly, the shape of PLNc was also described as rod-like, with an average length × width of the PLNc of approximately 150.68 ± 42.10 nm × 6.52 ± 0.96 nm, respectively (Figure 8c-d). Additionally, comparing the dimensions of the PLNc in the current research with other studies, it was found that Chawalitsakunchai et al. (2021) successfully obtained an average length and width of PLN as 130.02 ± 48.55 × 5.14 ± 2.03 nm, while Santos et al. (2013) obtained 249.7 ± 51.5 × 4.45 ± 1.41 nm. However, the dimensions of the nanocellulose reported were different in length depending on the conditions of hydrolysis, raw materials, the procedure of extractions, as well as other factors.

Table 2 summarized the length and diameter of nanocellulose including aspect ratio measured using ImageJ software. The aspect ratio (L/d), which is the length divided by the diameter of the fiber, affects the fibers' reinforcing capacity. An aspect ratio with a higher value will result in a larger surface area, resulting in better reinforcement effects (Silvério et al., 2013). In this study, it was found that CHNc had a 29.81 ± 9.09 L/D ratio, which is lower than those obtained by de Andrade et al. 2019 (40.86). The L/D ratio of PLNc was 23.84 ± 8.19, which is lower than CHNc. Additionally, comparing the aspect ratio of the PLNc in the current research with other studies, it was found that Prado and Spinace´ (2019) obtained a lower value for the aspect ratio (L/D of 9). In general, the isolation of nanocellulose through acid hydrolysis from lignocellulosic biomass sources (e.g., cotton, flax, and jute) results in rod-like or short nanocrystals with an aspect ratio ranging from 16 to 50 (Amiralian et al., 2017). A high aspect ratio of nanocellulose can be produced in large quantities

and fabricated directly into film films with high strength, modulus, lightness, thermal stability, and optical transparency (Ryu et al., 2019). According to Shanmugam et al. (2021), nanocellulose films with higher aspect ratios tend to have lower water vapor permeability, an important factor when applying nanocellulose to food packaging (Nadeem et al., 2022).

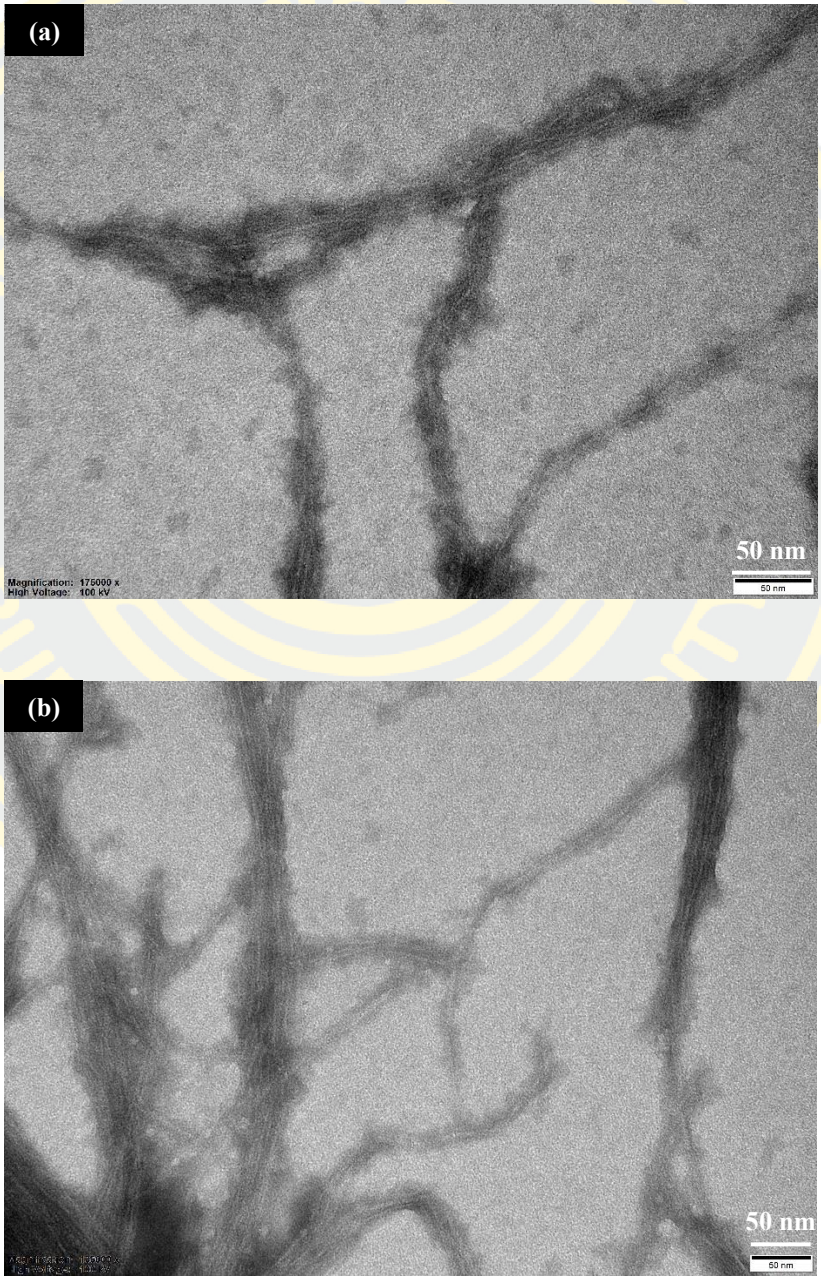

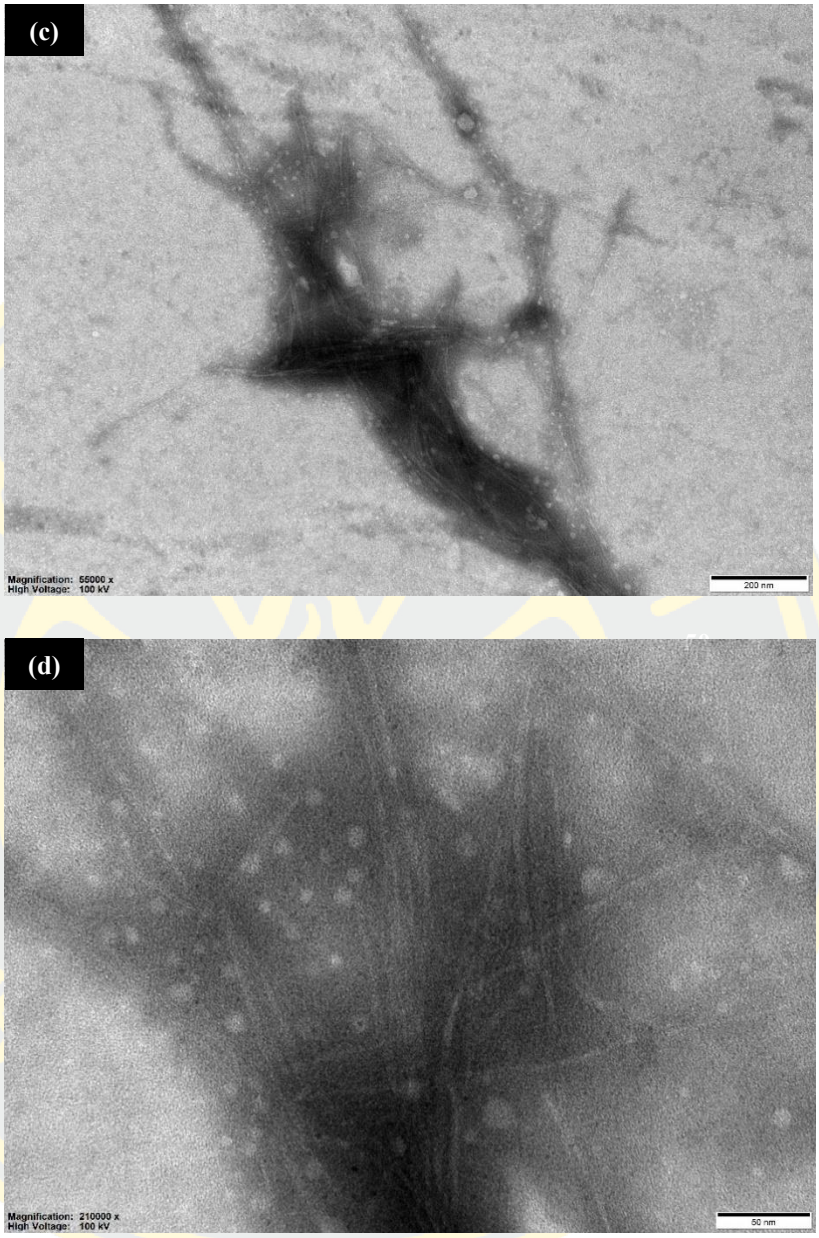

Figure 8 TEM images of nanocellulose (a) CHNc with 175000X (b) CHNc with 135000X (c) PLNc with 55000X (d) PLNc with 210000X.

Table 2 The size of nanocellulose

Nanocellulose	Length (nm)	Diameter (nm)	L/D ratio
CHNc	206.45 ± 41.09	7.24 ± 1.38	29.81 ± 9.09
PLNc	150.68 ± 42.11	6.52 ± 0.96	23.84 ± 8.19

X-ray Diffraction (XRD)

The X-ray patterns of the untreated CH, CHC, and CHNc are presented in Fig. 9(a) while the X-ray patterns of the untreated PL, PLC, and PLNc are illustrated in Fig. 9 (b). All samples showed crystalline peaks at 2θ = 15.6-16.5°, 21.8-22.0° and 34.5-34.7, corresponded to the (110), (200), and (004) planes respectively, which are characteristic of the cellulose Iβ structure (Feng et al., 2015). This observation also indicates that the crystalline structure of cellulose Iβ was maintained after alkali treatment, bleaching and acid hydrolysis. The calculated crystallinity index (CI) of the samples is shown in Table 3. The CI values of the untreated CH, CHC, CHNc are 32.76, 57.04, and 63.94%, respectively whereas the CI values of the untreated PL, PLC, PLNc are 46.01, 58.50, and 62.27%, respectively. The increased CI values for the extracted cellulose (CHC and PLC) and nanocellulose (CHNc and PLNc) as compared to the untreated CH and PL could be related to the effective removal of lignin and hemicellulose by alkali treatment and bleaching process.

The X-ray patterns of the untreated DH, DHC, CMC_{DH}, and CMC_{com} are shown in Fig. 9(c). The untreated DH and DHC showed crystalline peaks at 2θ = 15.7°, 22.0° and 35° which are characteristic of the cellulose Iβ structure. The calculated crystallinity index (CI) of the samples is shown in Table 3. The CI values of the untreated DH and DHC are 37.23 and 59.46%, respectively. The increased CI values for the extracted durian husk cellulose (DHC) could be ascribed to the effective removal of lignin and hemicellulose by alkali treatment and bleaching process. Additionally, the CI values of the CMC_{DH} and CMC_{com} decreased from 59.46 to 47.70% and 57.25%, respectively. As a result of the alkalization of NaOH during carboxymethylation reaction, molecules can be reorganized or completely cleaved (Klunklin et al., 2020).

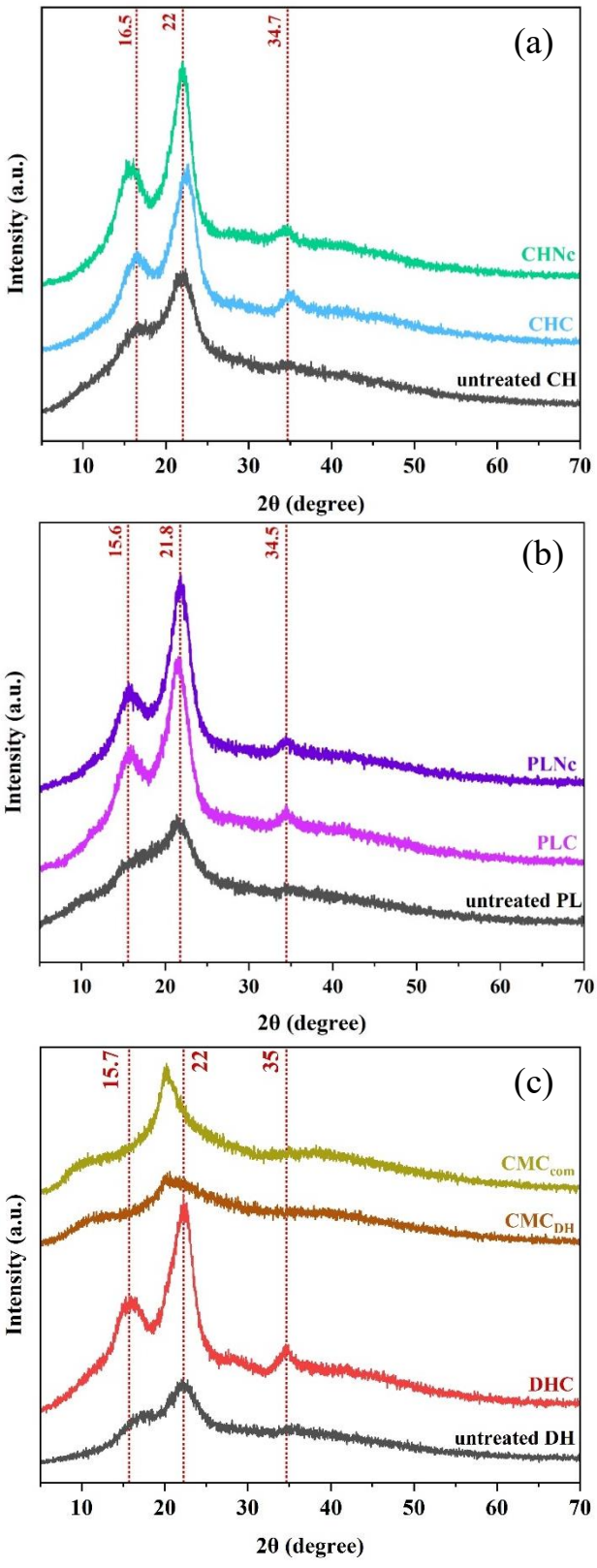
(a)
16.5
22
34.7
CHNc
CHC
untreated CH
Intensity (a.u.)
2θ (degree)
(b)
15.6
21.8
34.5
PLNc
PLC
untreated PL
Intensity (a.u.)
2θ (degree)
(c)
15.7
22
35
CMC com
CMC DH
DHC
untreated DH
Intensity (a.u.)
2θ (degree)

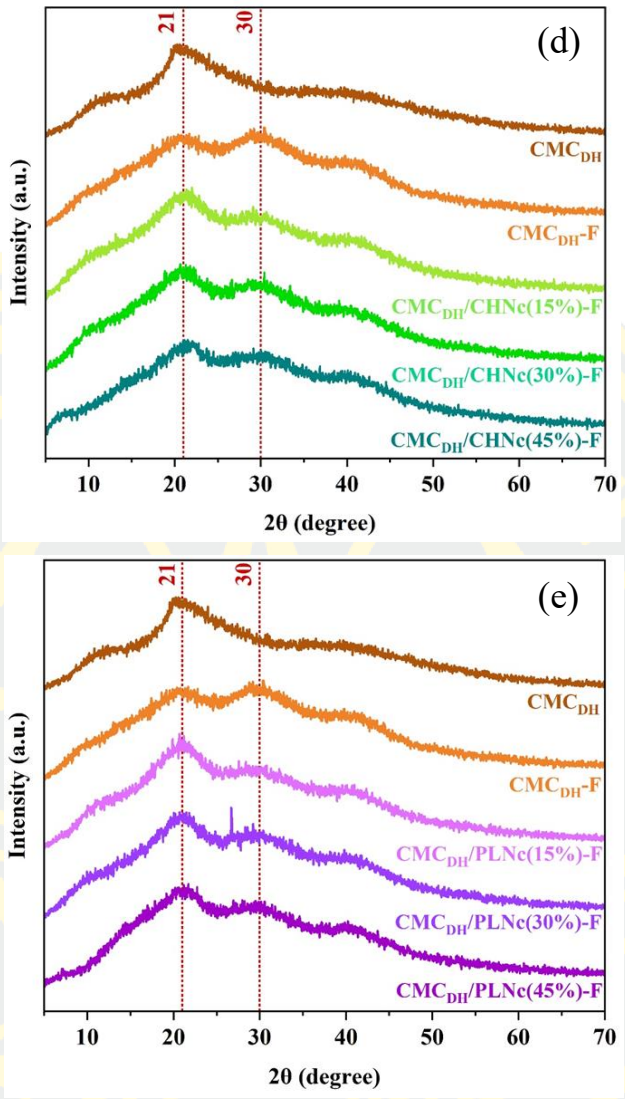

Figure 9 XRD patterns of (a) the untreated CH, CHC and CHNc, (b) untreated PL, PLC and PLNc, (c) untreated DH, DHC, CMC_{DH}, CMC_{com}, (d) CMC_{DH}, CMC_{DH}-F, CMC_{DH}/CHNc(15%)-F, CMC_{DH}/CHNc(30%)-F, and CMC_{DH}/CHNc(45%)-F, (e) CMC_{DH}/PLNc(15%)-F, CMC_{DH}/PLNc(30%)-F, and CMC_{DH}/PLNc(45%)-F.

Table 3 The crystallinity index of CHNc and PLNc

Materials	Crystallinity index (%)
Corn husks	
Untreated CH	32.76
CHC	57.04
CHNc	63.94
Pineapple leaves	
Untreated PL	46.01
PLC	58.50
PLNc	62.27
Durian husks	
Untreated DH	37.23
DHC	59.46
CMC_{DH}	47.70
CMC_{com}	57.25

The X-ray patterns of the prepared films of CMC_{DH}-F, CMC_{DH}/CHNc(15%)-F, CMC_{DH}/CHNc(30%)-F, and CMC_{DH}/CHNc(45%)-F, are shown in Fig. 9(d) whereas the X-ray patterns of the films of CMC_{DH}-F, CMC_{DH}/PLNc(15%)-F, CMC_{DH}/PLNc(30%)-F, and CMC_{DH}/PLNc(45%)-F are presented in Fig. 9 (e). For CMC_{DH}-F, two broad peaks with low intensity were observed at $2\theta = 21°$ and 29.5°°; however, its intensity at the peak $2\theta = 21°$ was noticeable lower than that of CMC_{DH}. This might be because the CMC_{DH}-F composed of glycerol as plasticizer. It was seen that the introduction of CHNc and PLNc in CMC_{DH} film slightly increased the intensity of crystalline peaks at $2\theta = 21°$ and slightly decreased the intensity of crystalline peaks at $2\theta = 29.5°$. The results showed that there was no difference in terms of crystallinity for the composite films with different type and amount of nanocellulose compositions.

Fourier Transform Infrared Spectroscopy (FTIR)

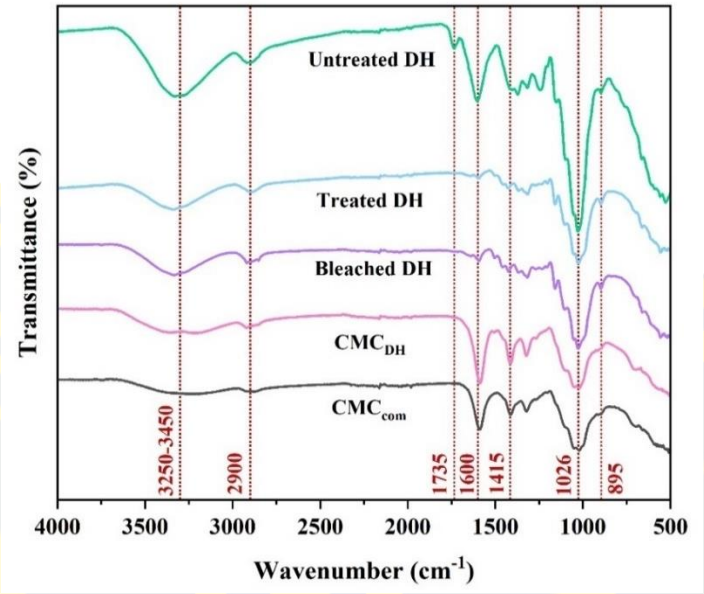

Figure 10 FTIR spectra of untreated durian husks (DH), treated DH, bleached DH, CMC_{DH}, and CMC_{com}.

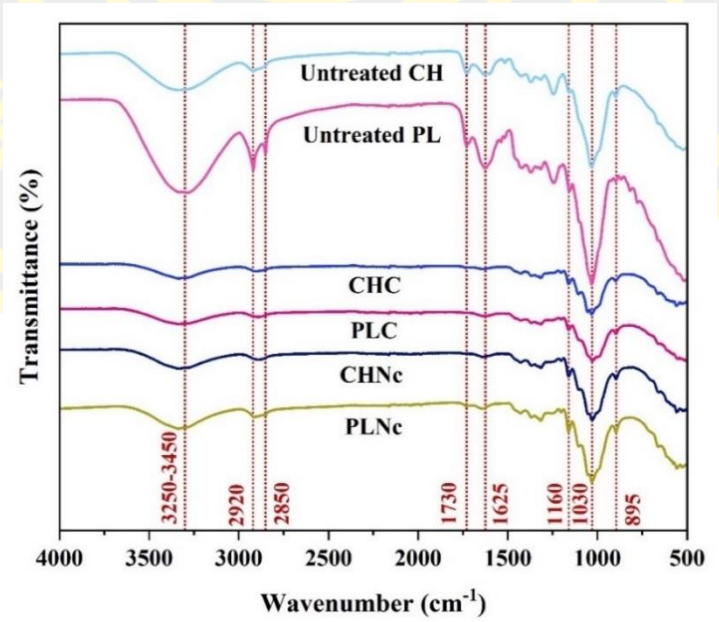

Figure 11 FTIR spectra of untreated corn husks (CH), untreated pineapple leaves (PL), CH cellulose (CHC), PL cellulose (PLC), CH nanocellulose (CHNc), and PL nanocellulose (PLNc).

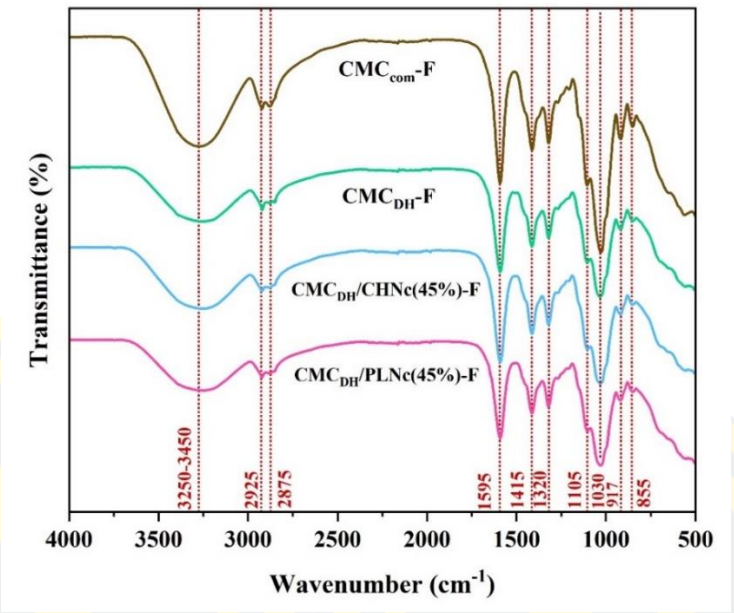

Figure 12 FTIR spectra of CMC_{com}-F, CMC_{DH}-F, CMC_{DH} /CHNc(45%)-F, and CMC_{DH} /PLNc(45%)-F.

The alkaline treatment can remove wax, oil, some lignin, and hemicellulose from the surface of fiber. This alkaline treatment also disrupts the hydrogen bonding, depolymerize cellulose, extract lignin and hemicellulose, as well as reduce the hydroxyl (OH^-) groups from the fiber by ionizing them to the alkoxide (RO^-) (Li et al., 2007). In this way, the hydrophilicity of natural fibers can be reduced, and the compatibility between natural fibers and polymer matrix could be improved. The FTIR spectra of untreated durian husks (DH), treated DH, bleached DH, CMC_{DH}, and commercial CMC (CMC_{com}) are shown in Fig. 10. The DH showed a broad peak at 3250-3350 cm^{-1} and a weak peak at 2917 cm^{-1} due to O-H and C-H stretching within the cellulose molecule, respectively. Absorption peaks at 1600 cm^{-1} correspond to stretching vibrations of carboxyl compounds (COO^-), whereas absorption peaks at 1438 cm^{-1} correspond to stretching vibrations of carboxyl compounds in salt form (COO^-Na) (Hidayat et al., 2018). The peak at 1734 cm^{-1} observed in the DH (or untreated DH) describes the acetyl and ester groups in hemicellulose or lignin (Santos et al., 2013). Compared with untreated DH, treated and bleached DH had totally disappeared hemicellulose and lignin peaks at 1734 cm^{-1}. Therefore, these results indicate that alkaline and bleaching treatments effectively removed non-cellulosic

components. Additionally, the absorption band of the hydroxyl group stretching, which appears at 3300–3400 cm^{-1}, in treated and bleached DH decreases compared to the untreated DH. This suggests that there is a possibility of the hydroxyl group being replaced by a carboxymethyl group. Hence, the presence of a novel carbonyl group stretching peak at 1584 cm^{-1} and CH_2 scissoring peak at 1415 cm^{-1}clearly indicates an increase in these groups in CMC (Klunklin et al., 2021). CMC_{DH}'s FTIR spectrum is similar to that of CMC_{com}, indicating that this study was successful in synthesizing CMC from durian rinds.

The FTIR spectra of untreated corn husks (CH), untreated pineapple leaves (PL), CH cellulose (CHC), PL cellulose (PLC), CH nanocellulose (CHNc), and PL nanocellulose (PLNc) are shown in Fig. 11. Similar to untreated DH, untreated CH and PL showed a broad peak at 3250-3350 cm^{-1} and a weak peak at 2920 cm^{-1} due to O-H and C-H stretching within the cellulose molecule, respectively. The peak at 1730 cm^{-1} observed in the untreated CH and PL is described to the acetyl and ester groups in hemicellulose component or lignin. Compared with the untreated CH and PL, the peak at 1730 cm^{-1} was found to decreased in cellulose (CHC and PLC) and nanocellulose (CHNc and PLNc) due to the removal of hemicellulose and lignin. The obtained CHNc and PLNc showed higher peak intensity than CHC and PLC at 1040 cm^{-1} and 895 cm^{-1}, implying that the higher relative content of cellulose (Dai et al. 2018). Additionally, FTIR spectra of CHNc and PLNc were like that of CHC and PLC in all wavenumbers, suggesting the non-destruction of the main cellulose structure (Feng et al., 2015). There was no difference between FTIR spectra of different agricultural wastes providing they were undergone similar treatments.

The FTIR spectra of CMC_{com} film, CMC_{DH} film, CMC_{DH}/CHNc(45%) film, and CMC_{DH}/PLNc(45%) film are shown in Fig. 12. The broad peak observed in all the films between 3000 and 3400 cm^{-1} refers to the O-H stretching vibration, while the peak at 2925 cm^{-1} is attributed to the C-H stretching vibration (Kulkarni et al., 2011), similar to the observation made on raw agricultural residues, cellulose, and nanocellulose discussed earlier. At 1595 cm^{-1}, absorption peaks correspond to stretching vibrations of carboxyl compounds (COO^-), and at 1415 cm^{-1}, to stretching vibrations of carboxyl compounds in salt form (COO^-Na) (Hidayat et al., 2018). In spite of the fact that these bands were not observed in CHNc and PLNc, they were

observed in CMC_{DH} composite films due to the absorption bands observed at 1600 cm^{-1} and 1415 cm^{-1} in CMC_{DH}. There were no noticeable peaks different from those of the constituent components in the CMC_{DH} /PLNc(45%) and CMC_{DH} /CHNc(45%) films, suggesting that no chemical reaction took place between CMC_{DH} and the nanocellulose (CHNc and PLNc) throughout the production of the biocomposite film (Dai et al., 2018).

Thickness, Color values, and Transmittance

The thickness of biocomposite films is measured using a Mitutoyo Digital Indicator Thickness Gauge and displayed in Table 4. It is found that the thickness of composite films ranged from 0.10 to 0.12 mm. Compared to neat CMC_{DH}-F, the thickness of neat CMC_{com}-F was lower. An increase in the concentration of CHNc and PLNc slightly increased thickness of the CMC_{DH} and CMC_{com} composite films. Despite the bigger sizes of CHNc, CMC_{DH}/PLNc composite films at the same nanocellulose concentration were marginally thicker than CMC_{DH}/CHNc composite films.

Table 4 Thickness of biocomposite films

Films	Thickness (mm)
CMC_{DH}-F	0.0980 ± 0.0045^{a}
CMC_{DH}/CHNc(15%)-F	$0.1040 \pm 0.0114^{a,b}$
CMC_{DH}/CHNc(30%)-F	$0.1100 \pm 0.0141^{a,b}$
CMC_{DH}/CHNc(45%)-F	0.1140 ± 0.0114^{b}
CMC_{DH}/PLNc(15%)-F	$0.1060 \pm 0.0089^{a,b}$
CMC_{DH}/PLNc(30%)-F	0.1160 ± 0.0114^{b}
CMC_{DH}/PLNc(45%)-F	0.1180 ± 0.0084^{b}
CMC_{com}-F	0.0820 ± 0.0084
CMC_{com}/CHNc(45%)-F	0.0840 ± 0.0089
CMC_{com}/PLNc(45%)-F	0.0840 ± 0.0134

Mean ± Standard deviation values within a column in the same group followed by the different letters (a–b) are significantly different ($p < 0.05$)

The appearances of biocomposite films and CIE L*a*b* color values are shown in Fig.13 and Table 5, respectively. CMC_{com} film and CMC_{com} composite films were clearer and stickier compared to the CMC_{DH} film and composite films prepared in this experiment. The wrinkle shown in Fig. 13 of the CMC_{com} film and CMC_{com} composite films were due to the films' stickiness, and it was hard to remove the films from petri dish. The clearness or transparency of the films can be seen from the high value of L* (closed to 100) and very low a* and b* values (closed to zero). In addition, whiteness index (WI) of the films was closed to 100. However, the appearances of the CMC_{DH} film as well as the composite films prepared from CHNc and PLNc in the range of nanocellulose concentration between 15-45% w/w were indistinguishable observed with naked eyes and in general more opaque and yellowish in color compared with CMC_{com} film and CMC_{com} composite films.

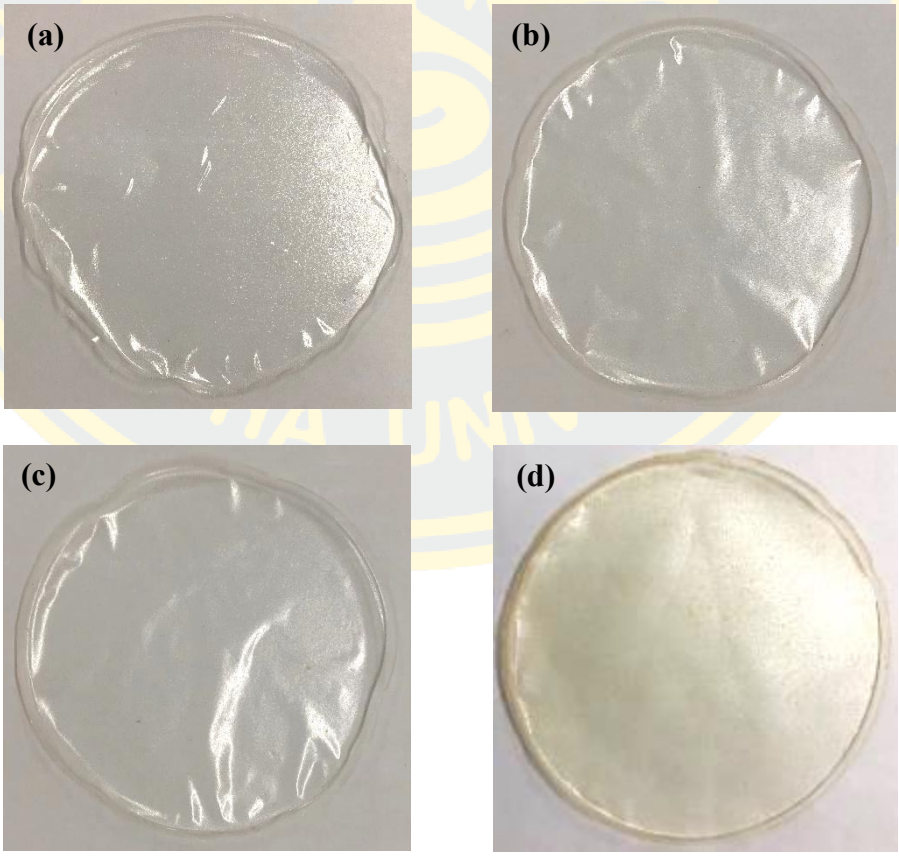

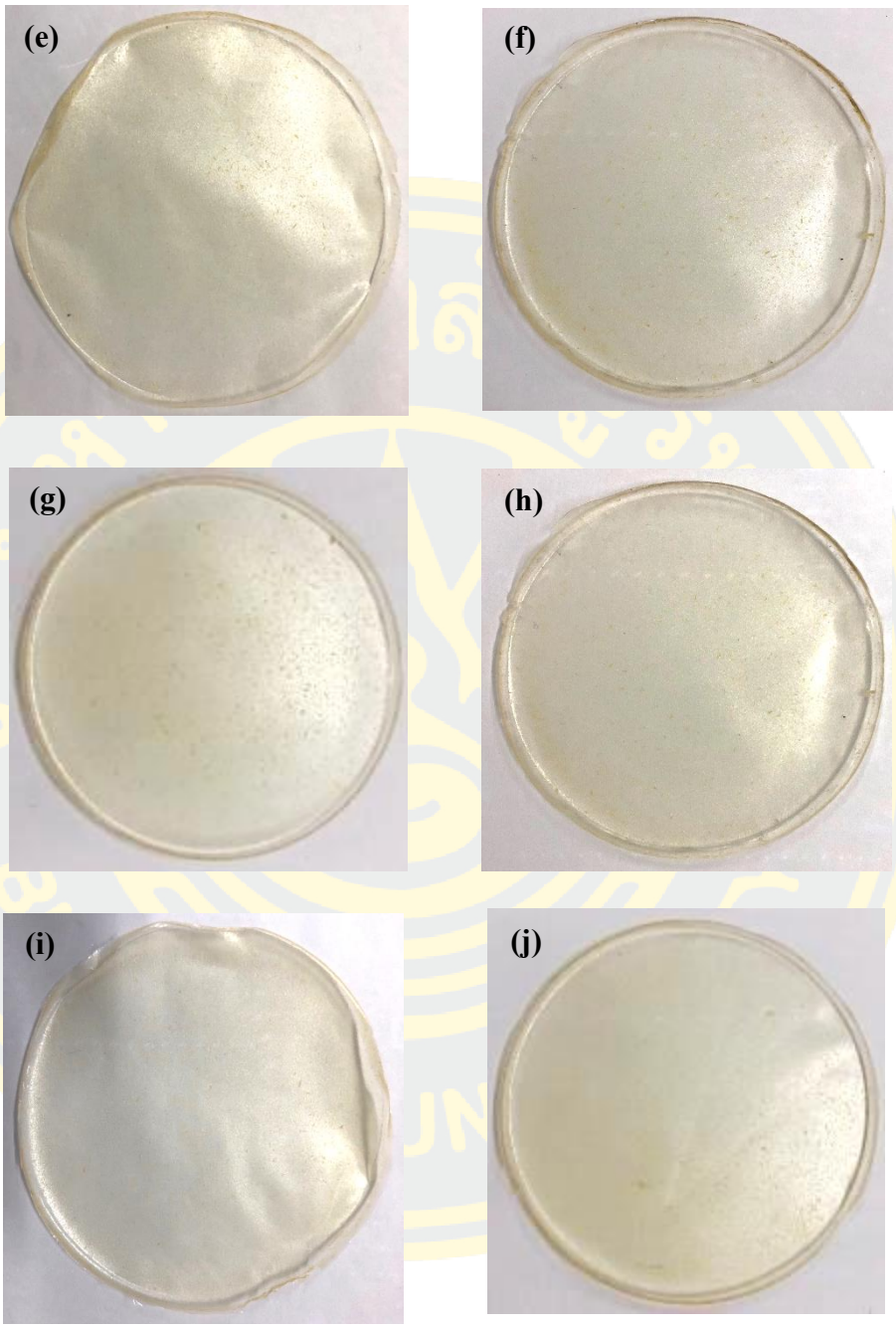

Figure 13 Appearance of (a) CMC_{com} film (b) CMC_{com}/CHNc(45%) (c) CMC_{com}/PLNc(45%) (d) CMC_{DH} film (e) CMC_{DH}/CHNc(15%) (f) CMC_{DH}/CHNc(30%) (g) CMC_{DH} /CHNc(45%) (h) CMC_{DH}/PLNc(15%) (i) CMC_{DH}/PLNc(30%) (j) CMC_{DH} /PLNc(45%).

Table 5 presents the color values of the composite films including the L* [lightness; between 0 (black) and 100 (white)], a* [red–green; + = redder, - = greener], b* [yellow–blue; + = yellower, - = bluer] and whiteness index (WI) [0 = black, 100 = white]. The color of the films is a significant physical property that can easily be observed, so when selecting films for packaging purposes, the color should be considered. It was obvious that CMC_{DH} film prepared in this research had a high positive b* value, suggesting yellowish in color. This might be due to the remaining pigments in the extracted cellulose. This caused the biofilm and biocomposite films prepared in this work has yellowish appearance compared to CMC_{com} film and composite films. As expected, since b* values were high, WI of the CMC_{DH} film was only 79.17, significantly lower than WI value of 99.67 of the CMC_{com} film. It was discovered that biocomposite films reinforced with CHNc and PLNc exhibit a lower L* value or reduced lightness when compared to neat CMC_{DH} film. Moreover, the a* and b* values of biocomposite films was slightly altered from the neat CMC_{DH} film, in which a* marginally decreased and b* increased, when incorporating with nanocellulose. As the PLNc are darker in color than the CHNc, the composite films incorporating with PLNc possessed lower WI than those incorporating with CHNc. An increase in nanocellulose composition resulted in an increase in b* value and hence a decrease in WI of the nanocomposite films.

Table 5 Color values of biocomposite films

Films	Color value			WI
	L*	a*	b*	
CMC_{DH}-F	99.97 ± 0.06^{a}	-1.30 ± 0.00^{a}	5.63 ± 0.06^{a}	79.17 ± 0.15^{a}
CMC_{DH}/CHNc(15%)-F	98.40 ± 0.00^{d}	-1.30 ± 0.00^{a}	6.93 ± 0.06^{b}	73.70 ± 0.17^{b}
CMC_{DH}/CHNc(30%)-F	99.67 ± 0.06^{b}	-1.47 ± 0.06^{b}	7.13 ± 0.06^{c}	73.87 ± 0.35^{b}
CMC_{DH}/CHNc(45%)-F	99.20 ± 0.00^{c}	-1.50 ± 0.00^{b}	7.73 ± 0.06^{d}	71.50 ± 0.17^{c}
CMC_{DH}/PLNc(15%)-F	98.20 ± 0.00^{e}	-1.80 ± 0.00^{d}	7.20 ± 0.00^{c}	72.83 ± 0.06^{d}
CMC_{DH}/PLNc(30%)-F	99.97 ± 0.06^{a}	-1.50 ± 0.00^{b}	8.00 ± 0.00^{e}	69.70 ± 0.00^{e}
CMC_{DH}/PLNc(45%)-F	99.90 ± 0.00^{a}	-1.60 ± 0.06^{c}	8.47 ± 0.06^{f}	69.70 ± 0.17^{e}
CMC_{com}-F	99.27 ± 0.06	0.10 ± 0.00	-0.70±0.00	99.67 ± 0.06
CMC_{com}/CHNc(45%)-F	99.53 ± 0.06	- 0.70 ± 0.00	-0.10±0.00	97.73 ± 0.06
CMC_{com}/PLNc(45%)-F	99.70 ± 0.00	- 0.70 ± 0.06	-0.20±0.00	98.20 ± 0.00

Data with the different letter in a column are significantly different ($p \leq 0.05$)

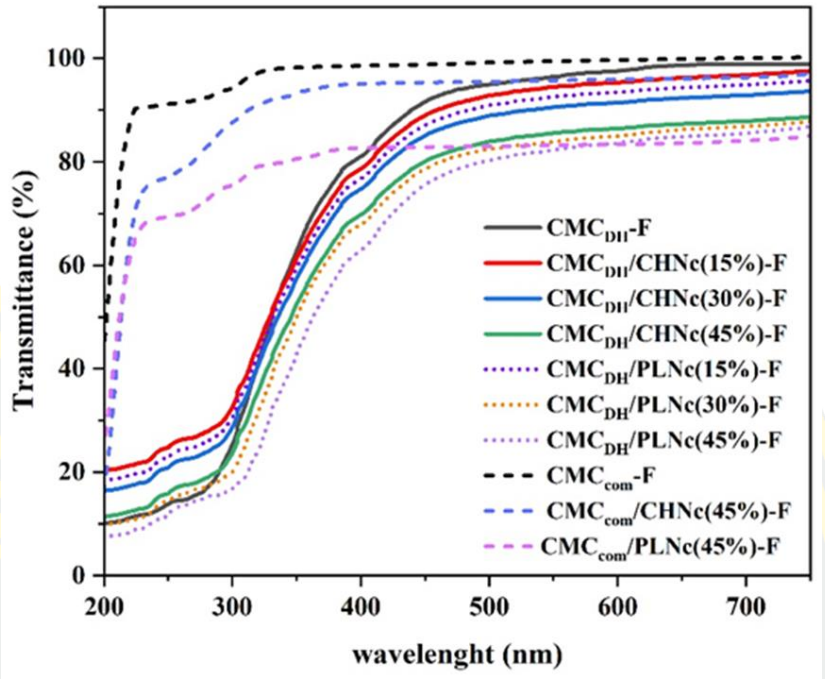

Figure 14 Light transmittance of composite films.

The transparency of the films can also be seen from the transmittance spectra in the UV−visible range of 200−800 nm as seen in Figure 14. It can be noticed that CMC_{com} film was fully transmitted to light in the UV-visible wavelength with the perfect percent transparency of 100% although the light transmitted in the UV range was slightly lower than that in the visible range. When 45% w/w CHNc and PLNc were added into the CMC_{com} film, degree of transmittance was decreased to around 95 and 80%, respectively, although they were still transmitted to the entire UV-visible wavelength with a lower degree on the transmittance in an UV range compared to that in a visible range. On the other hand, CMC_{DH} film was transmitted only in the visible range, however, the precent transmittance in the range of 600-700 nm was closed to 100% similar to the that of the CMC_{com} film. Compared with the neat CMC_{DH} film, the transmittance of CMC_{DH}/CHNc and CMC_{DH}/PLNc decreased with increasing the concentration of nanocellulose, suggesting that addition of nanocellulose in the CMC_{DH} film decreased the transparency of the films. It is possible that the high concentration of CHNc and PLNc in CMC_{DH} matrix contributes to the particle aggregate phenomenon, which results in scattering and reduced transparency (Ma et

al., 2011). Similar to CMC_{com} composite films, PLNc had a stronger effect on light transmittance reduction than CHNc in CMC_{DH} composite films despite the fact that PLNc was smaller in size than CHNc. Nevertheless, the lowest percent transmittance of CMC_{DH}/PLNc(45%) composite film was considerably high and comparable to that of CMC_{com}/PLNc(45%) at 80%.

Scanning Electron Microscope (SEM)

The morphology of biocomposite films was investigated by SEM to investigate the nanocellulose distribution, as shown in Figure 15. The results showed that the neat CMC_{DH} film was homogeneous and smooth, without any aggregates. After adding CHNc and PLNc, the surface of the biocomposite films becomes rougher and more inhomogeneous, with small aggregates on the film surface. A low concentration of nanocellulose was observed to be better dispersed in the CMC_{DH} composite film. It was observed that a CHNc content of 30% and 45% resulted in an inhomogeneous film surface with small agglomerates. In addition, CMC_{DH}/PLNc(45%) exhibited an inhomogeneous, but larger agglomerate than CMC_{DH}/PLNc(15%) and CMC_{DH}/PLNc(30%). A similar observation was also reported for biocomposite films reinforced with pineapple crown nanocellulose. During the preparation of biocomposite films (sonication for 45 minutes), the dispersion of nanocellulose was insufficient to reverse agglomeration (Benini et al., 2020).

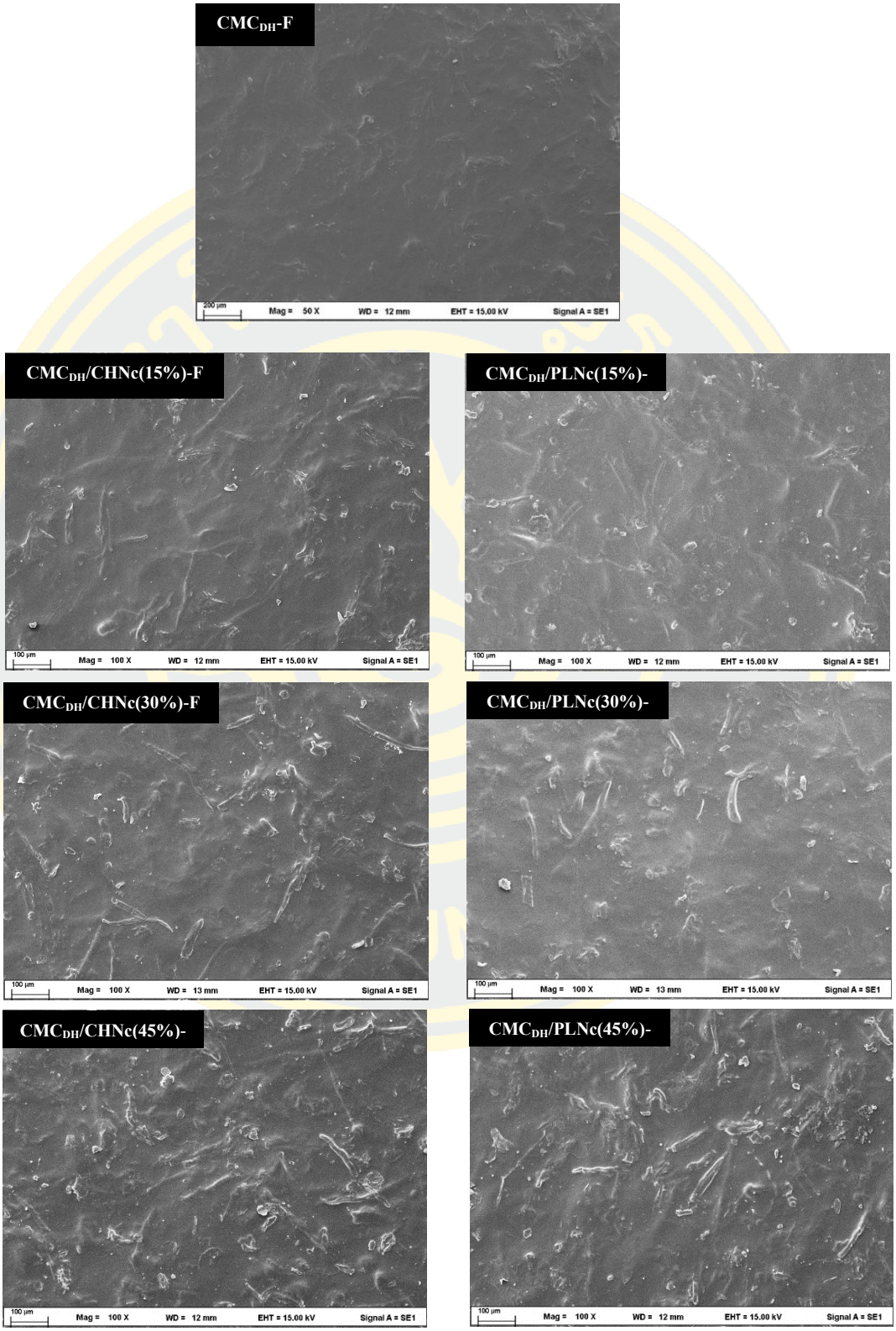

Figure 15 SEM images of neat CMC_{DH} film and CMC_{DH} composite films.

Mechanical properties

The effect of nanocellulose on the mechanical properties of biocomposite films are shown in Fig. 16-18. Figure 16 (a) represents the tensile strength (TS) of the neat CMC_{DH} film, CMC_{DH}/CHNc, and CMC_{DH}/PLNc films. The neat CMC_{DH} film showed the lowest tensile strength as compared to the CMC_{DH}/CHNc and CMC_{DH}/PLNc films. The TS value increased with increasing CHNc content. With the addition of 45% of CHNc gave the highest tensile strength (4.521 MPa). The same trend was found from the research on the PVA composite film reinforced with nanocellulose from coconut fibers (Yusmaniar et al., 2023). After increasing the content of PLNc, the TS value initially increased from 1.60 MPa (neat CMC_{DH}) to 4.90 MPa (15% addition of PLNc) and 5.07 MPa (30% addition of PLNc), and then decreased to 3.78 MPa (45% addition of PLNc). PLNc aggregates in the CMC_{DH} matrix due to Van der Waal's forces, resulting in the relatively decreased TS value of the CMC_{DH}/PLNc film (Haafiz et al., 2014). Savadekar and Mhaske (2012) also observed that higher concentrations of nanocellulose in films would result in larger agglomerates, poor particle distribution, and phase separation (Savadekar & Mhaske, 2012). Furthermore, the decrease in TS value at higher loading content of nanocellulose can be explained by a reduction in the compatibility between matrix and nanocellulose (Zhou et al., 2017). Figure 16 (b) represents the comparison of TS value between the CMC_{com} and CMC_{DH} biocomposite films. The results showed that the TS value of the neat CMC_{com} film was higher than the neat CMC_{DH} film. Moreover, after reinforcing 45% of CHNc and 30% of PLNc, the tensile properties of CMC_{DH} biocomposite film was higher than the CMC_{com} biocomposite film.

The highest strength achieved in this study was 4.52 MPa for CMC_{DH}/CHNc(45%) and 5.06 for CMC_{DH}/PLNc(30%), which was higher than that reported by Dai et al. (3.25 MPa) but was still lower than the one developed by Xiao et al. (55.56 MPa) (Dai et al., 2018b; Xiao et al., 2016). This variation might be attributed to variances in the molecular weight, filler type, and fiber source of the NCCs produced in this study. In this study, TS was lower in comparison to synthetic packaging. According to Su and Zhang, high-density polyethylene has a TS of 29.3 MPa (Su & Zhang, 2016). Rhim et al. found polypropylene is 31 -38 MPa (Rhim et al., 2013). Boldt et al. found low-density polyethylene is 20 MPa (Boldt et al., 2016).

The elongation at break (EB) of the biocomposite films are shown in Figure 17 (a-b). The EB value of the biocomposite films was increased with that incorporating CHNc and PLNc. However, the EB of CMC_{DH}/CHNc decreased with increasing CHNc content. Figure 17 (b) represents the comparison of the EB between the CMC_{com} and CMC_{DH} biocomposite films. The results showed that the EB of the neat CMC_{com} film was higher than the neat CMC_{DH} film. Moreover, after reinforcing 45% of CHNc and 30% of PLNc, the EB of CMC_{com} biocomposite film was higher than the CMC_{DH} biocomposite film. Earlier reports also showed that adding nanocellulose to composite films increased TS and decreased EB value. The same trend was found from the research on the WPI composite film reinforced with nanocellulose from pineapple crown leaf (F. Fitriani et al., 2021) and the Gellan gum composite film reinforced with pineapple peel nanocellulose (Dai et al., 2018b).

The toughness of the biocomposite films exhibited a similar trend with the tensile strength results of the CMC_{DH}/CHNc and CMC_{DH}/PLNc films, as shown in Figure 18 (a-b). The toughness increased with increasing CHNc content. With the addition of 45% of CHNc gave the highest toughness (1.22 MJ/m^3). Moreover, after reinforcing PLNc into the CMC_{DH} matrix, the toughness increased sharply, and the toughness increased with increasing PLNc content from 15% to 30%. With the addition of 30% of PLNc gave the highest toughness (1.95 MJ/m^3). Figure 18 (b) indicates the comparison of the toughness between the CMC_{com} and CMC_{DH} biocomposite films. The results showed that the toughness of the neat CMC_{com} film was higher than the neat CMC_{DH} film. However, after reinforcing 45% of CHNc and 30% of PLNc, the toughness of CMC_{DH} biocomposite film was higher than the CMC_{com} biocomposite film.

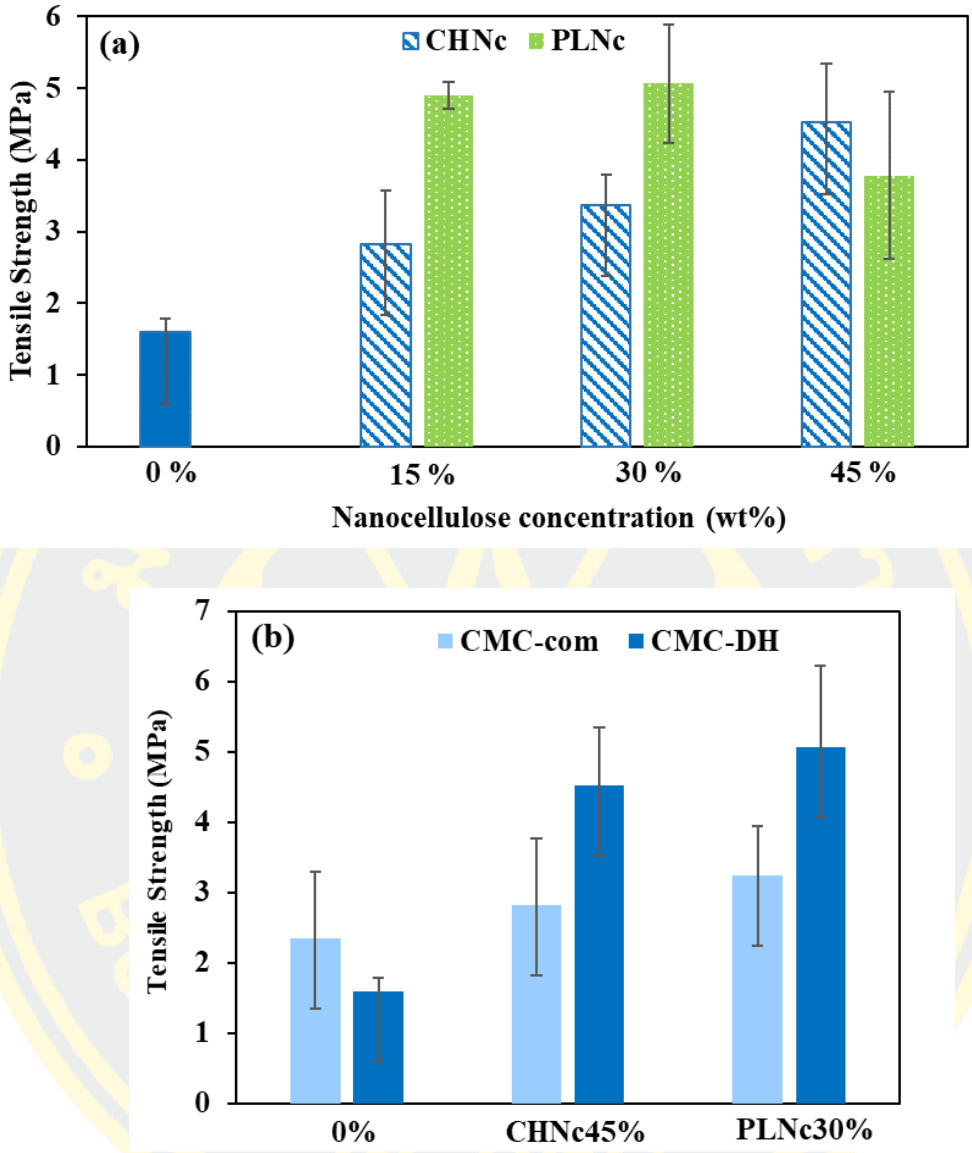

Figure 16 Tensile strength of (a) CMC_{DH} composite films (b) CMC_{com} composite films.

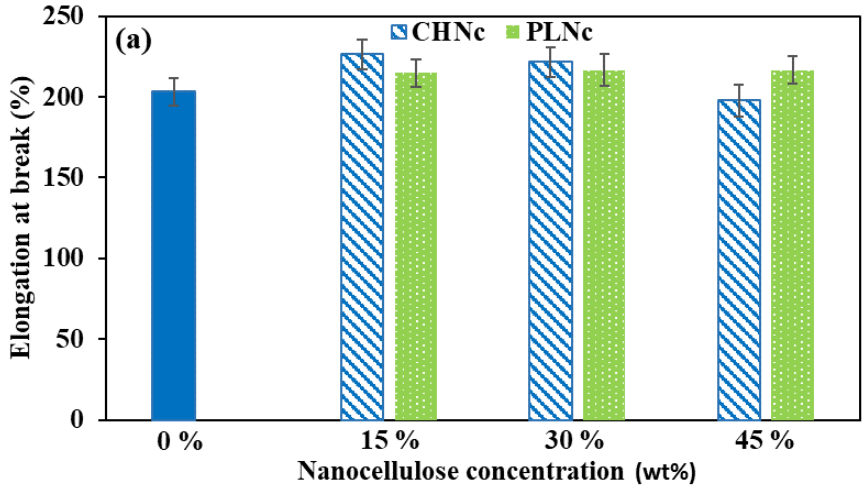

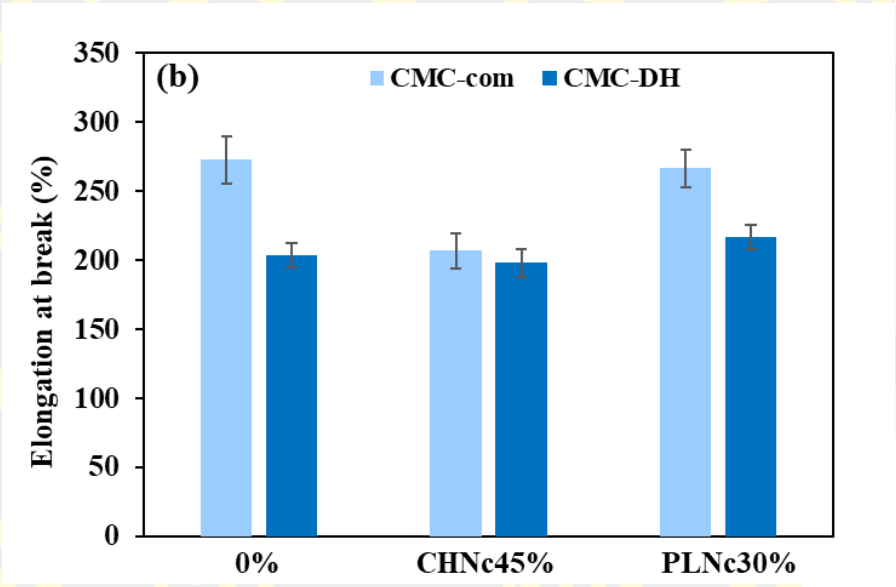

Figure 17 Elongation at break of (a) CMC_{DH} composite films (b) CMC_{com} composite films.

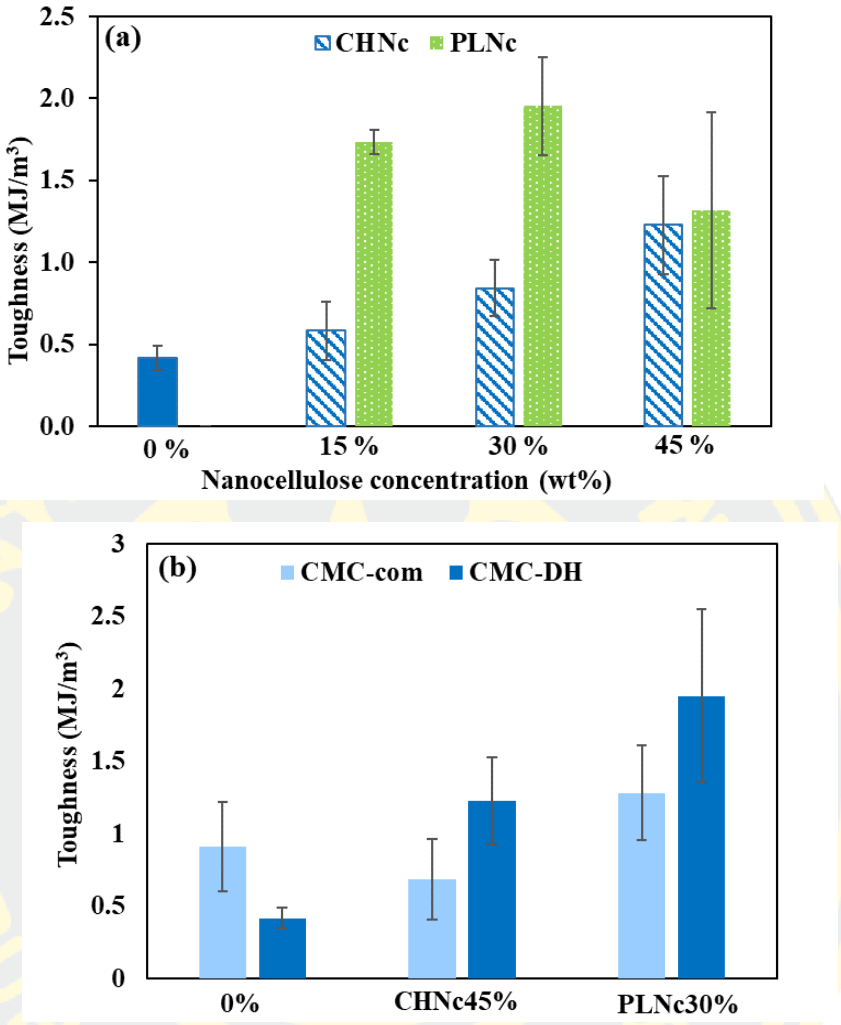

Figure 18 Toughness of (a) CMC_{DH} composite films (b) CMC_{com} composite films.

Thermogravimetric analysis (TGA)

Figure 19 (a-b) illustrates the TGA and DTG curves of CMC_{DH}, CHNc, CMC_{DH}-F, and CHNc-reinforced CMC_{DH} composites at different nanocellulose contents. Figure 20 (a–b) shows the TGA and DTG curves of PLNc, CMC_{DH}-F, and CMC_{DH} composites reinforced with PLNc at different nanocellulose contents. The thermal data are presented in Table 6, including the onset temperature (T_{onset}), 50% film weight loss temperature ($T_{50\%}$), maximum degradation temperature (T_{max}), and the percentage of material residues at 600°C. In Fig. 19(a) and 20(a), an initial weight loss shown in all samples in the range of 40-150°C, corresponding to decomposition stage I in Fig. 19(b) and 20(b), due to the evaporation of absorbed water. It can be

clearly seen that the moisture contents in CMC_{DH}, CHNc, and PLNc were around 5-10% w/w, significantly lower than those of the films due to the fact that the composite films were prepared by using water as a solvent as well as contained glycerol as plasticizer. The moisture contents of the films were considerably high at 26% for CMC_{DH}-F, 18-28% for CMC_{DH}/CHNc-F, and 22-24% for CMC_{DH}/PLNc-F. When comparing CMC_{DH} with CHNc and PLNc, it was revealed that CMC_{DH} contained a higher moisture content because CMC_{DH} has a lower crystallinity than nanocellulose, which indicates that CMC_{DH} has more space to retain water molecules due to its hydrophilic character (confirmed by XRD data) (Mandal & Chakrabarty, 2011).

In the second region (II) in Fig. 19(b) and 20(b), weight loss occurred between 150 to 210°C with the neat CMC_{DH} film as well as the CMC_{DH}/CHNc film, and CMC_{DH}/PLNc composite films. These weight loss of less than 7% was attributed to the volatilization of plasticizer (Zarina, 2015).

Mass reduction at the third region (III) in Fig. 19(b) and 20(b) occurred at 250 to 400°C, corresponding to the degradation of CMC and nanocellulose. The weight loss in this region was 38% for CMC_{DH}, 77% for CHNc, 70% for PLNc, 37-42% for CMC_{DH}/CHNc, and 39-40% for CMC_{DH}/PLNc. The addition of nanocellulose both CHNc and PLNc resulted in a slight increase in the onset temperature of the neat CMC_{DH} film from 179°C to around 184-186°C for CHNc and to 182-188°C. This indicates that CHNc and PLNc improved the thermal stability of the CMC_{DH} biocomposite films. While $T_{50\%}$ was also increased about 10°C when nanocellulose was incorporated into the neat CMC_{DH} film, insignificant changes of T_{max} were observed. The low residues of around 10% of nanocellulose at 600°C suggested its high purity while the ash content of CMC_{DH} and CMC_{DH}-F at 600°C was as high as 42% and 23%, respectively. Despite the fact that nanocellulose decomposes almost perfectly well, once the nanocellulose was added into the neat CMC_{DH} film, the residues at 600°C slightly increased to around 25-28%. In general, there was no noticeable difference in thermal behavior of the composite films containing CHNc and PLNc in the range of 15-45% w/w. Shankar and Rhim (2016) concluded that the superior thermal stability of the composite films containing nanocellulose might be attributed to a strong contact between the CMC_{DH} matrix and nanocellulose .

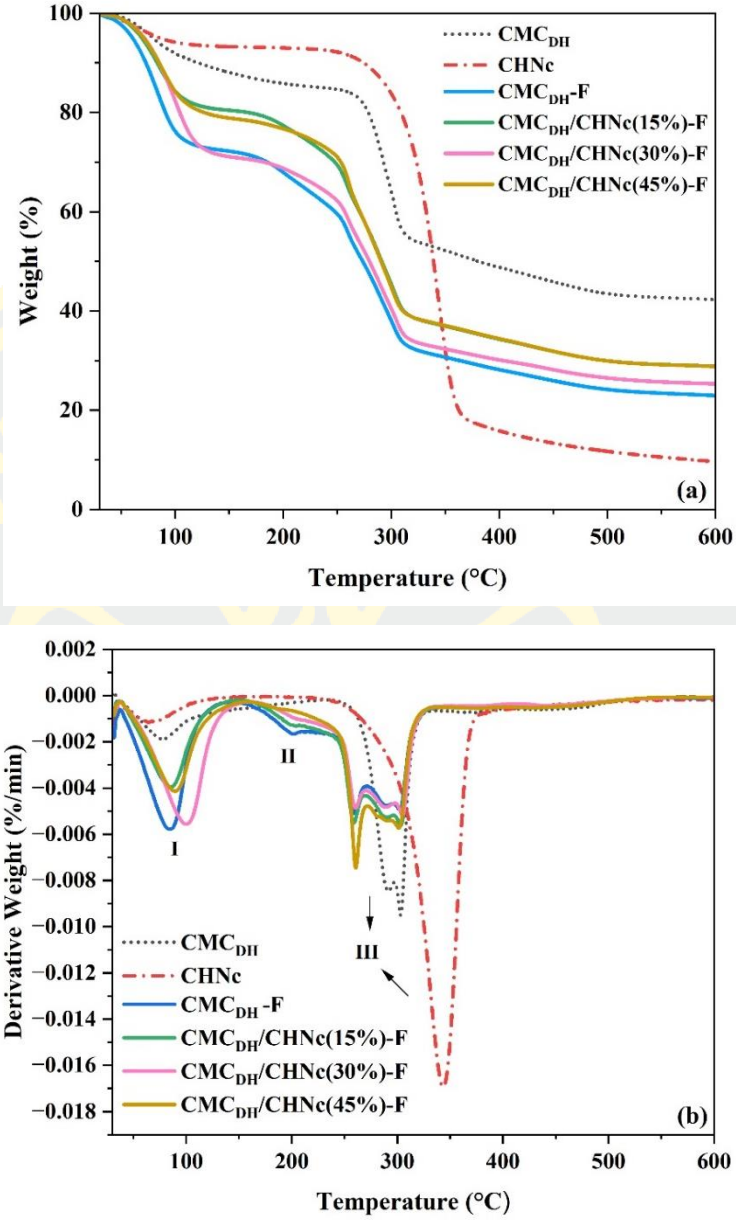

Figure 19 (a) TGA and (b) DTG profiles of CMC_{DH}, CHNc, neat CMC_{DH}-F and its composite film.

Table 6 Thermal degradation data of CMC_{DH} film reinforced with CHNc

Materials	T_{onset} (°C)	$T_{50\%}$ (°C)	T_{max} (°C)	Residue (%) at 600 °C
CMC_{DH}	274.23	380.84	303.09	42.33
CHNc	289.71	339.19	343.37	9.69
CMC_{DH}-F	179.27	273.68	259.92	22.98
CMC_{DH} /CHNc(15%)-F	186.43	291.14	258.85	28.89
CMC_{DH} /CHNc(30%)-F	184.73	279.81	260.40	25.34
CMC_{DH} /CHNc(45%)-F	185.70	290.53	260.66	28.84

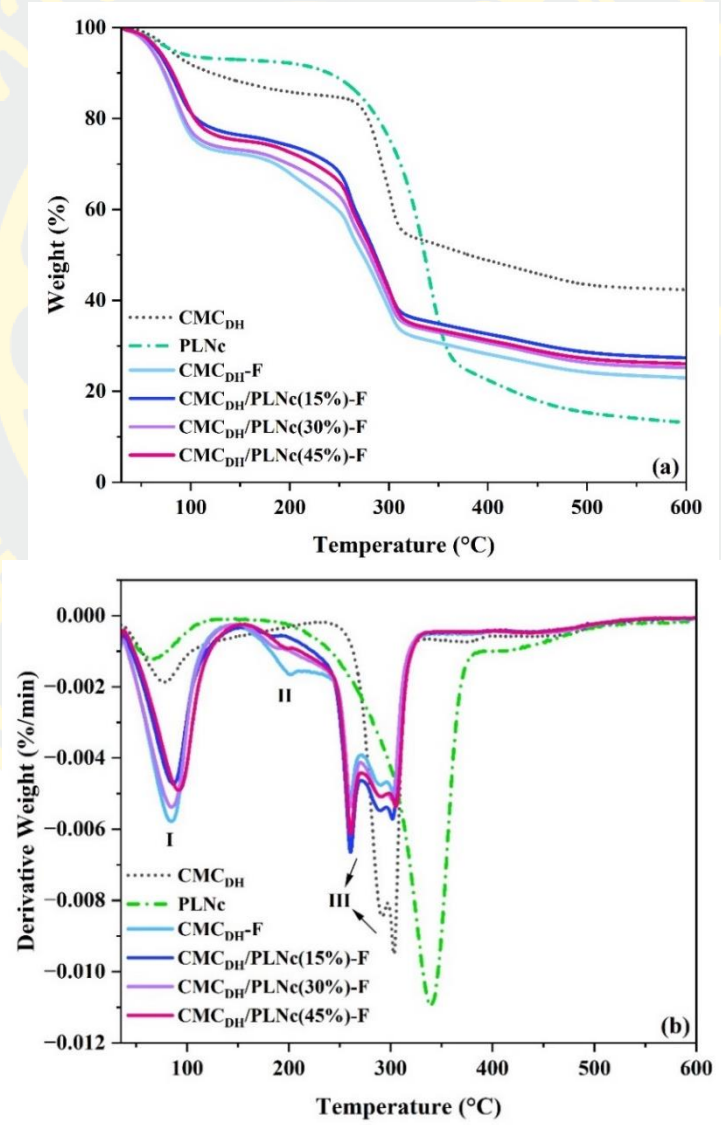

Figure 20 (a) TGA and (b) DTG profiles of CMC_{DH}, PLNc, neat CMC_{DH}-F and its composite film.

Table 7 Thermal degradation data of CMC_{DH} film reinforced with PLNc

Materials	T_{onset} (°C)	$T_{50\%}$ (°C)	T_{max} (°C)	Residue (%) at 600 °C
CMC_{DH}	274.23	380.84	303.09	42.33
PLNc	261.88	336.06	339.18	13.14
CMC_{DH}-F	179.27	273.68	259.92	22.98
CMC_{DH} /PLNc(15%)-F	187.58	286.24	260.63	27.37
CMC_{DH} /PLNc(30%)-F	184.49	280.42	261.29	25.23
CMC_{DH} /PLNc(45%)-F	182.47	284.52	260.92	26.07

Differential Scanning Calorimetry (DSC)

Figure 21 shows the DSC diagram of CMC_{DH}, CHNc, PLNc, neat CMC_{DH} film, CMC_{DH}/CHNc, and CMC_{DH}/PLNc composite films at different nanocellulose concentrations. The characteristics of composite films including melting temperature (T_m) and maximum degradation temperature (T_{dm}) are summarized in Table 8. The first endothermic peak was found between 70 and 150 °C in all samples, attributed to the evaporation of water and in agreement with TGA results (Gazonato et al., 2019). The second endothermic transition occurred at temperatures around 250-260°C were observed for the neat and composite films. This might be due to the evaporation of glycerol using as plasticizer in the films, corresponding to thermal transition stage II in TGA results. The exothermic peaks at 320-380 °C, representing the decomposing temperature, were in agreement with the third region (III) of TGA thermal transition. It can be seen that CMC_{DH} decomposed at the lowest temperature with the peak temperature at 290 and 320 °C. The two decomposition peaks of CMC_{DH} suggested that there might be other components remaining after the extraction process. On the other hand, nanocellulose disintegrated at the highest temperatures of 356 and 347°C for CHNc and PLNc, respectively. The peak decomposition temperature of neat CMC_{DH} film was at 316°C. When incorporating nanocellulose into the neat CMC_{DH} film, the decomposition temperatures increased slightly to around 320-325°C, suggesting thermal stability enhancement. The decomposition temperatures of the composite films prepared from CHNc and PLNc at different nanocellulose concentrations were not distinguishable.

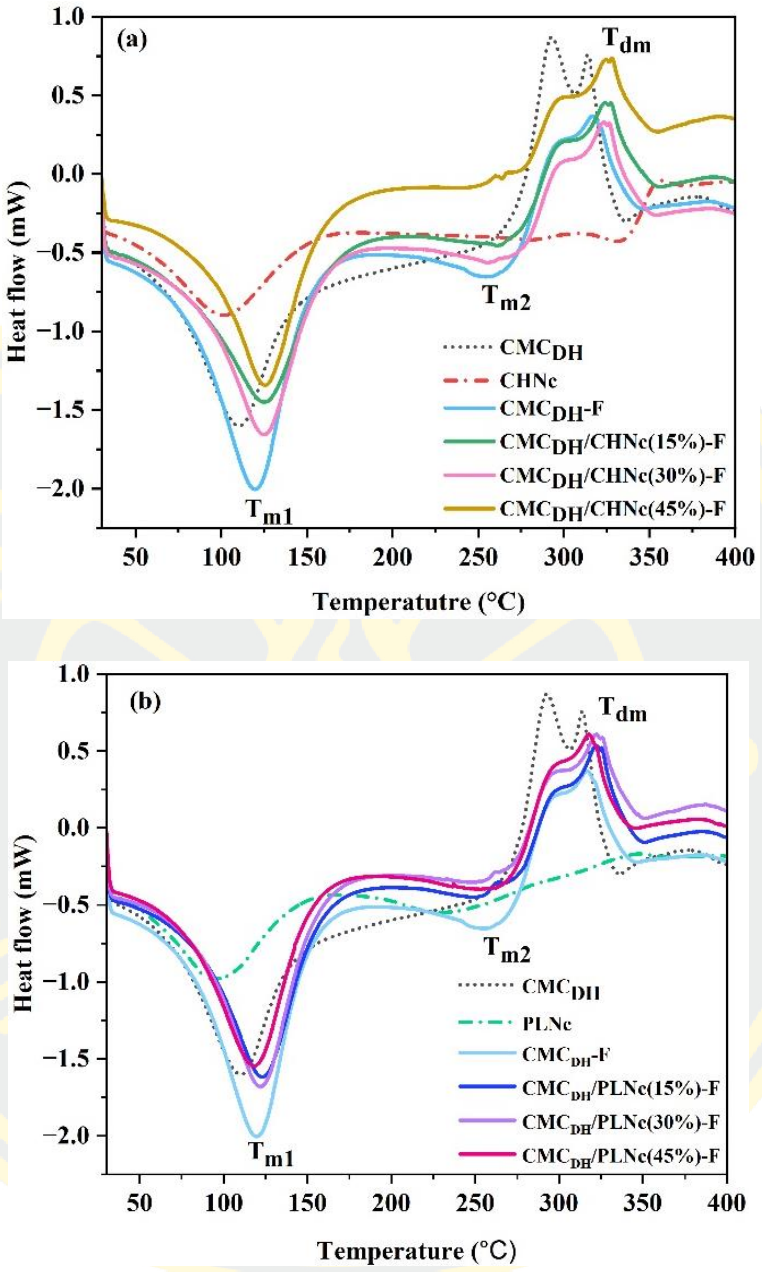

Figure 21 DSC diagram of (a) CMC_{DH}, CHNc, neat CMC_{DH} film and CMC_{DH}/CHNc composite films (b) PLNc and CMC_{DH}/PLNc composite films.

Table 8 DSC data of CMC_{DH}/CHNc composite films

Materials	T_{m1} (°C)	T_{m2} (°C)	T_{dm} (°C)
CMC_{DH}	110.28	-	292.83
CHNc	101.94	-	356.53
PLNc	96.24	-	347.67
CMC_{DH}-F	119.74	254.65	316.97
CMC_{DH} /CHNc(15%)-F	125.35	261.17	324.15
CMC_{DH} /CHNc(30%)-F	124.91	258.22	323.51
CMC_{DH} /CHNc(45%)-F	125.81	263.92	324.71
CMC_{DH} /PLNc(15%)-F	123.19	250.50	321.82
CMC_{DH} /PLNc(30%)-F	122.52	254.68	322.45
CMC_{DH} /PLNc(45%)-F	119.30	257.52	318.02

Water vapor transmission rate (WVTR)

The water vapor transmission rates (WVTR) of biocomposite films are shown in Figure 22(a). The results indicated that the WTVR of CMC_{DH} biocomposite films decreased with increasing nanocellulose content. With the addition of 15 and 30%of CHNc, the WVTR decreased from 2.77 to 2.70 and 2.33 $g/m^2 \cdot h$, respectively. With the addition of 15 and 30% of PLNc, the WVTR decreased from 2.77 to 2.34 and 2.10 $g/m^2 \cdot h$, respectively. These results indicate that adding nanocellulose (CHNc and PLNc) decreased the WVTR value, indicating an increased resistance to the transmission of water vapor. Due to the strong hydrogen bonding interaction between the nanocellulose and matrix, the adhesion of the material is enhanced. Additionally, nanocellulose has a high crystallinity, which has a positive effect on water vapor barrier properties, as diffusion and adsorption mostly occur in amorphous regions (Xu et al., 2024). However, the water vapor transmittance increased to 2.36 and 2.20 $g/m^2 \cdot h$ with adding 45% of CHNc and PLNc, respectively. The presence of agglomerates could be the result of the increase in WVTR due to the limit of the uniformity and compactness of the polymers by reducing the total surface area available for bonding (Shahi et al., 2020).

Figure 22 (b) indicates the comparison of the WVTR between the CMC_{com} and CMC_{DH} biocomposite films. The results showed that the WVTR of the neat CMC_{com} film was lower than the neat CMC_{DH} film, indicating an increased resistance to the transmission of water vapor. Moreover, after reinforcing 45% of CHNc and

30% of PLNc, the WVTR of CMC_{com} biocomposite film was lower than the CMC_{DH} biocomposite film.

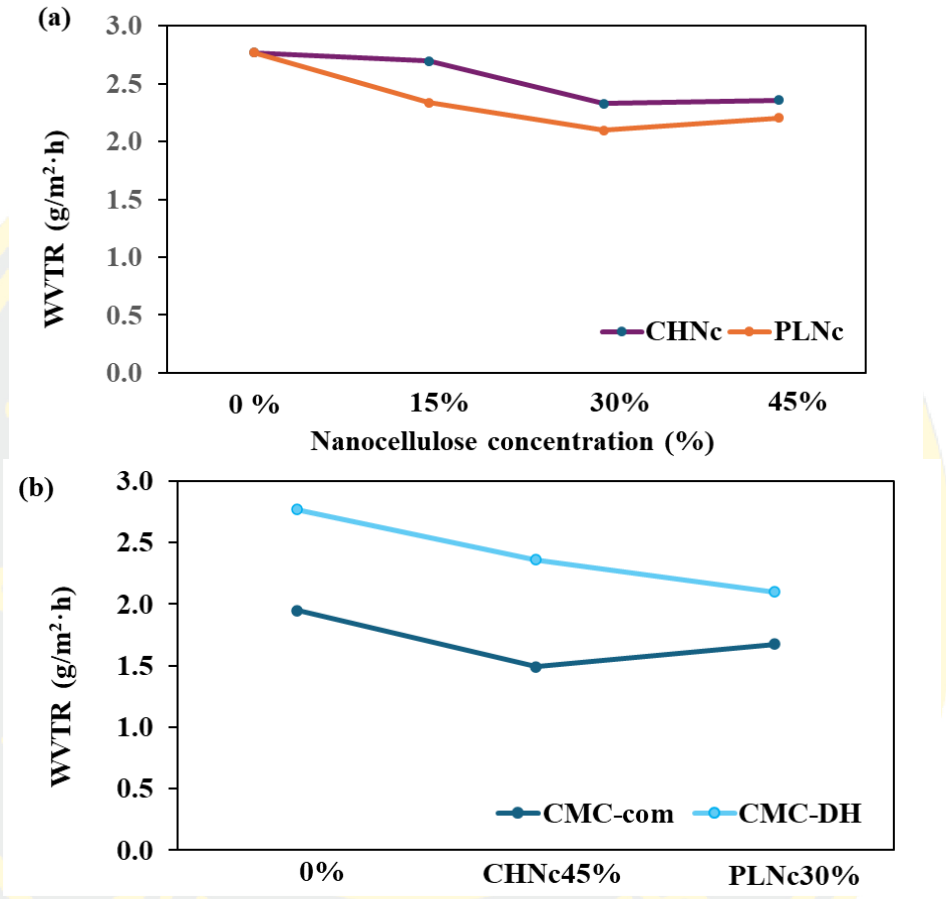

Figure 22 WVTR of (a) CMC_{DH} composite films and (b) CMC_{com} composite films.

Photodegradation

The optical appearance changes of the biocomposite films before and after UV light are shown in Fig. 23. The conditions initially were 75% relative humidity and a temperature of 30 °C. The results showed that the humidity decreased to 58% and the temperature increased to 55 °C after 7 days. After 2 days, all the films were hard and brittle as shown in Fig. 23. Moreover, the neat CMC_{com} film was out of shape after 6 days. Moreover, all samples did not change in color after 7 days of UV light exposure noticed by naked eyes. CMC_{DH} composite films prepared from different concentration of nanocellulose (CHNc and PLNc) exhibited no noticeable difference in photodegradability.

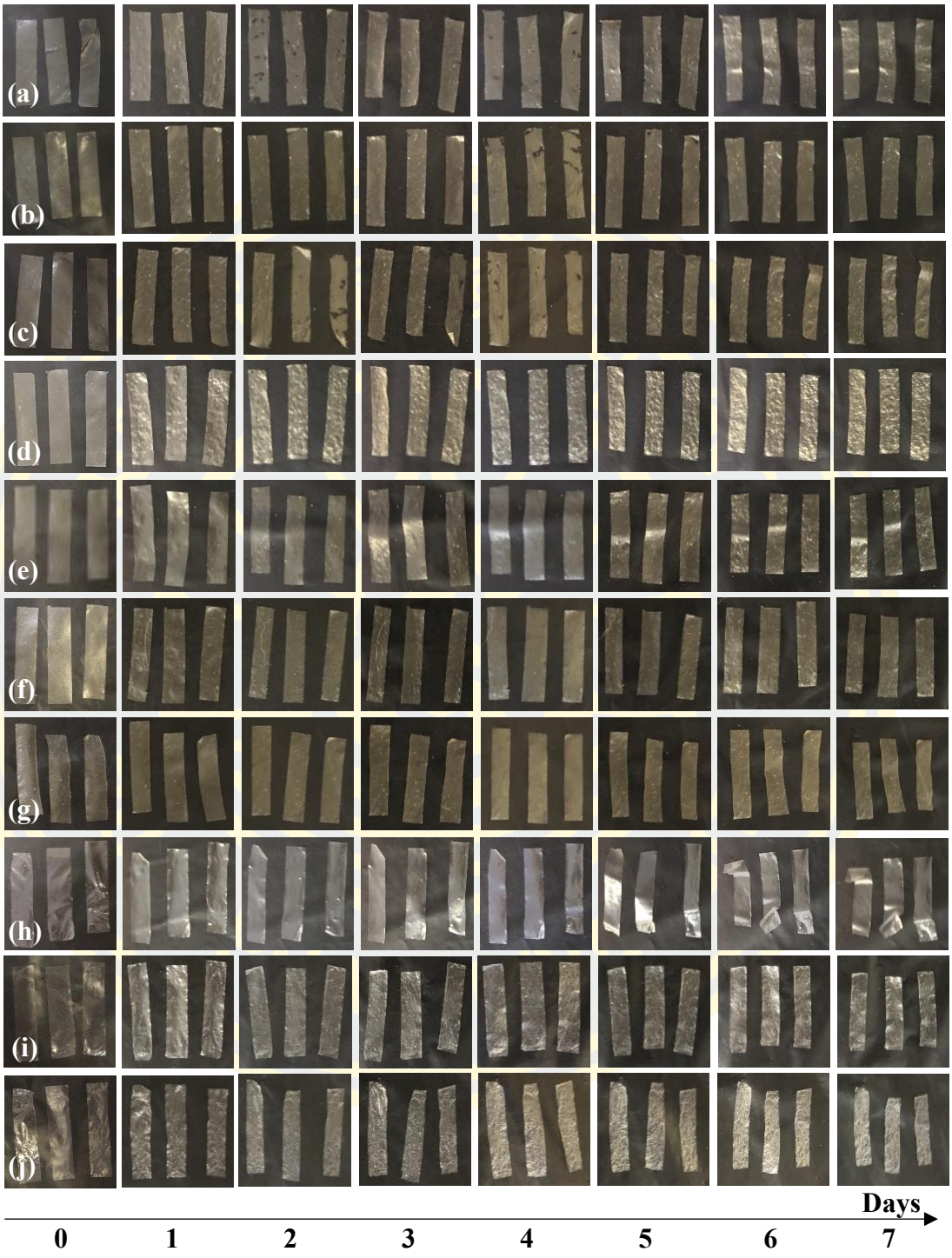

Figure 23 Appearance of biocomposite films after UV exposure (a) neat CMC_{DH} (b) CMC_{DH}/CHNc(15%) (c) CMC_{DH}/CHNc(30%) (d) CMC_{DH}/CHNc(45%) (e) CMC_{DH}/PLNc(15%) (f) CMC_{DH}/PLNc(30%) (g) CMC_{DH}/PLNc(45%) (h) neat CMC_{com} (i) CMC_{com}/CHNc(45%) (j) CMC_{com}/PLNc(30%).

Biodegradation

The physical appearance of biocomposite films after soil burial test for 0-3 days is shown in Figure 24. The films were buried in soil at 80% relative humidity at the beginning. The biodegradability of neat CMC_{com} and CMC_{DH} was completely within 2 days. CMC_{DH} composite films reinforced with nanocellulose (CHnc and PLNc) were completely degraded within 3 days, faster degradation rate than commercial synthetic plastic films. This result is consistent with the WVTR of CMC_{DH}/CHNc and CMC_{DH}/PLNc films, indicating that the reinforcement of nanocellulose prevented water from diffusing into the films (Bacha et al., 2022). Bacha et al. (2022) investigated the effect of nanocellulose on the biodegradation rate of PVA film and discovered that the higher the nanocellulose concentration, the slower the degradation. Zhao et al. 2019 investigated the biodegradability of cellulose films made from durian rind and discovered that the films were biodegraded in soil after 4 weeks (Zhao et al., 2019). In this study, there was no difference in biodegradability between CMC_{com} and CMC_{DH} composite films prepared from different concentration of nanocellulose (CHNc and PLNc).

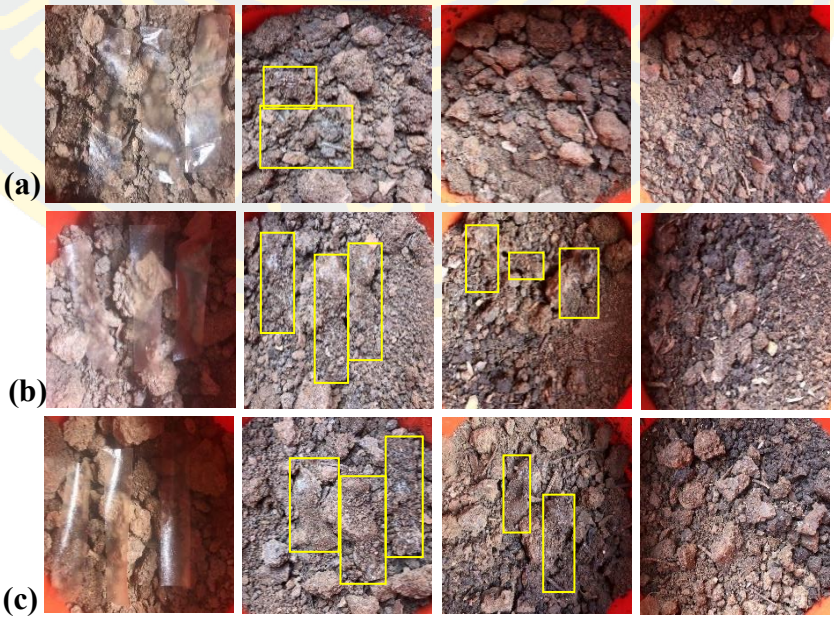

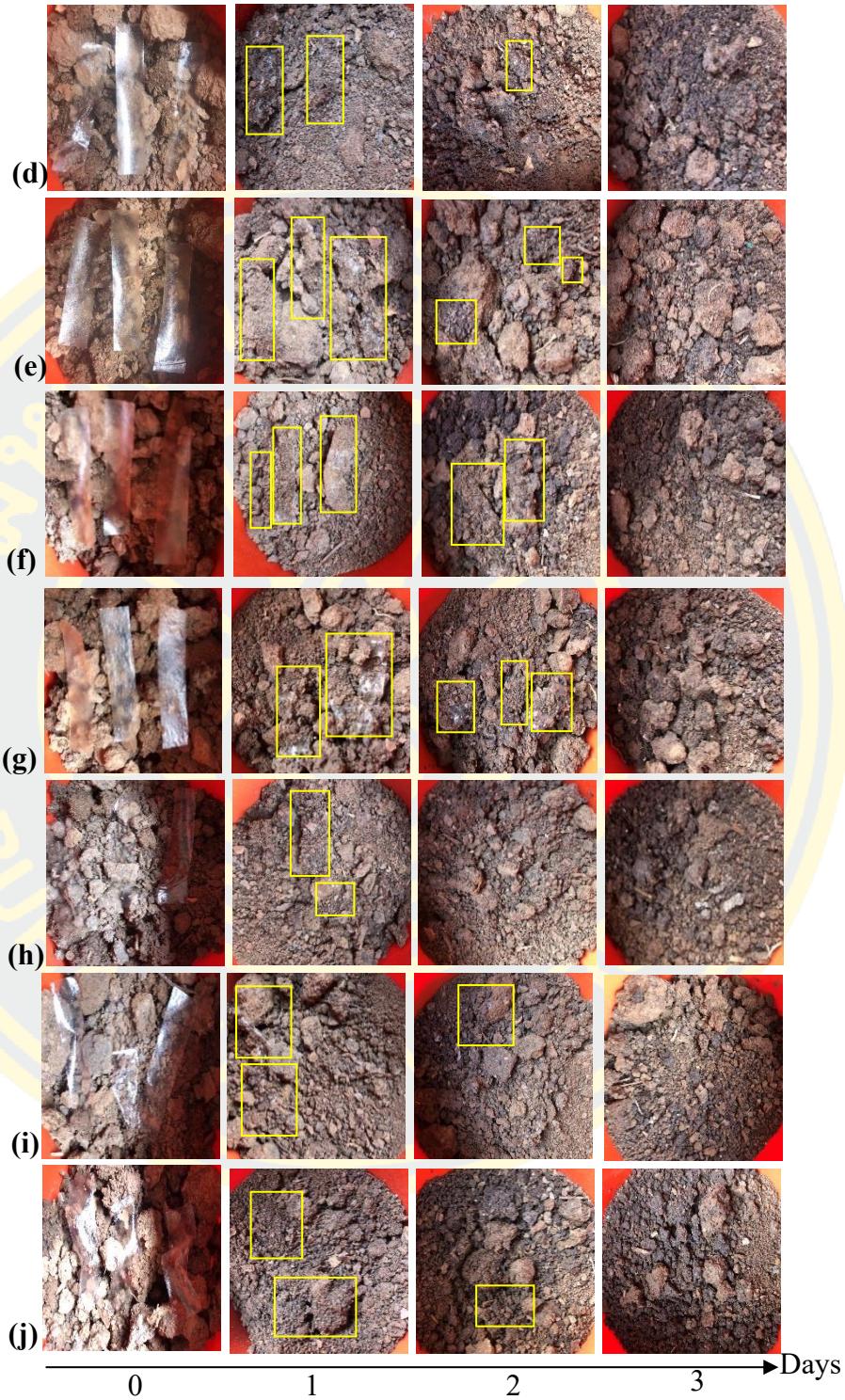

Figure 24 biodegradation of biocomposite films (a) neat CMC_{DH} (b) CMC_{DH}/CHNc(15%) (c) CMC_{DH}/CHNc(30%) (d) CMC_{DH}/CHNc(45%) (e) CMC_{DH}/PLNc(15%) (f) CMC_{DH}/PLNc(30%) (g) CMC_{DH}/PLNc(45%) (h) neat CMC_{com} (i) CMC_{com}/CHNc(45%) (j) CMC_{com}/PLNc(30%).

CHAPTER 5
CONCLUSION

Biocomposite film derived from agricultural wastes, i.e. durian husks, pineapple leaves, and corn husks, were successfully achieved. Carboxymethyl cellulose was prepared from durian husks (CMC_{DH}) through carboxymethylation process and utilized as a composite film matrix. Corn husks and pineapple leaves were treated with alkali and bleaching before being acid hydrolyzed to produce nanocellulose (CHNc and PLNc) and used as a reinforcement phase. The alkali and bleaching treatment effectively removed noncellulose components, including lignin and hemicellulose, according to XRD and FTIR data. With the treatments, CHNc showed an increase in the crystallinity index from 32.76% (untreated CH) to 62.27% (CHNc). For PLNc, the crystallinity index increased from 46.01% (untreated PL) to 63.94% (PLNc). Accord to TEM study, the obtained CHNc has a rodlike shape with an average length and diameter of 206.45 ± 41.10 nm and 7.24 ± 1.38 nm. The shape of PLNc was also described as rod-like, with an average length × width of the PLNc being approximately 150.68 ± 42.10 nm × 6.52 ± 0.96 nm. The composite films were prepared via solvent casting technique with different nanocellulose contents (15, 30, and 45 wt%). The addition of nanocellulose (CHNc and PLNc) reduced the transparency of the CMC_{DH} films but improved their water barrier, thermal stability, and tensile strength. The highest tensile strength was obtained from CMC_{DH}/PLNc(30%) with a value of 5.06 ± 0.83 MPa. CMC_{DH} composite films reinforced with nanocellulose (CHNc and PLNc) were completely degraded within 3 days during the soil burial, faster degradation rate than commercial synthetic plastic films. The research concept was influenced by the Thai government's Bio-Circular-Green (BCG) economic strategy. According to this study, agricultural wastes can be converted into value-added products. Incorporating nanocellulose (CHNc and PLNc) into CMC_{DH} films could enhance their properties and provide an attractive packaging alternative.

REFERENCES

Adinugraha, M., Marseno, D., & Haryadi. (2005). Synthesis and characterization of sodium carboxymethylcellulose from Cavendish banana pseudo stem (Musa cavendishii LAMBERT). *Carbohydrate Polymers, 62*, 164-169.

Al-Khanbashi, A., Al-Kaabi, K., & Hammami, A. (2005). Date palm fibers as polymeric matrix reinforcement: Fiber characterization. *Polymer Composites, 26*, 486-497.

Amiralian, N., Annamalai, P. K., Garvey, C., Jiang, E., Memmott, P., & Martin, D. (2017). High aspect ratio nanocellulose from an extremophile spinifex grass by controlled acid hydrolysis. *Cellulose, 24*.

Arnata, I., Harsojuwono, B., Hartiati, A., Anggreni, A., & Sartika, D. (2022). Effect of Alkaline Concentration Treatments on the Chemical, Physical and Thermal Characteristics of Cellulose from Tapioca Solid Waste. *Journal of Fibers and Polymer Composites, 1*, 117-130.

Arnata, I., Suprihatin, S., Fahma, F., Richana, N., & Sunarti, T. (2019). Cellulose Production from Sago Frond with Alkaline Delignification and Bleaching on Various Types of Bleach Agents. *Oriental Journal of Chemistry, 35*, 08-19.

Arrakhiz, F. Z., Elachaby, M., Bouhfid, R., Vaudreuil, S., Essassi, M., & Qaiss, A. (2012). Mechanical and thermal properties of polypropylene reinforced with Alfa fiber under different chemical treatment. *Materials & Design, 35*, 318-322.

Bacha, E. G., Demsash, H. D., Shumi, L. D., & Debesa, B. E. (2022). Investigation on Reinforcement Effects of Nanocellulose on the Mechanical Properties, Water Absorption Capacity, Biodegradability, Optical Properties, and Thermal Stability of a Polyvinyl Alcohol Nanocomposite Film. *Advances in Polymer Technology, 2022*, 6947591.

Beck-Candanedo, S., Roman, M., & Gray, D. G. (2005). Effect of Reaction Conditions on the Properties and Behavior of Wood Cellulose Nanocrystal Suspensions. *Biomacromolecules, 6*(2), 1048-1054.

Benini, K. C., Ornaghi, H., Medeiros, N., Pereira, P., & Cioffi, M. O. (2020). Thermal characterization and lifetime prediction of the PHBV/nanocellulose biocomposites using different kinetic approaches. *Cellulose, 27*.

Bledzki, A. K., & Jaszkiewicz, A. (2010). Mechanical performance of biocomposites

based on PLA and PHBV reinforced with natural fibres – A comparative study to PP. *Composites Science and Technology, 70*(12), 1687-1696.

Boldt, R., Gohs, U., Wagenknecht, U., & Stamm, M. (2016). Effect of electron-induced reactive processing on morphology and structural properties of high-density polyethylene. *Polymer, 95*, 1-8.

Casanova, F., Freixo, R., Pereira, C. F., Ribeiro, A. B., Costa, E. M., Pintado, M. E., & Ramos, Ó. L. (2023). Comparative Study of Green and Traditional Routes for Cellulose Extraction from a Sugarcane By-Product. *Polymers, 15*(5).

Charoenvai, S. (2014). Durian Peels Fiber and Recycled HDPE Composites Obtained by Extrusion. *Energy Procedia, 56*, 539-546.

Chawalitsakunchai, W., Dittanet, P., Loykulnant, S., Sae-oui, P., Tanpichai, S., Seubsai, A., & Prapainainar, P. (2021). Properties of natural rubber reinforced with nano cellulose from pineapple leaf agricultural waste. *Materials Today Communications, 28*, 102594.

Chen, H., Zhang, W., Wang, X., Wang, H., Wu, Y., Zhong, T., & Fei, B. (2018). Effect of alkali treatment on wettability and thermal stability of individual bamboo fibers. *Journal of Wood Science, 64*(4), 398-405.

Collazo-Bigliardi, S., Ortega-Toro, R., & Chiralt, A. (2019). Using lignocellulosic fractions of coffee husk to improve properties of compatibilised starch-PLA blend films. *Food Packaging and Shelf Life, 22*, 100423.

Dai, H., Ou, S., Huang, Y., & Huang, H. (2018a). Utilization of pineapple peel for production of nanocellulose and film application. *Cellulose, 25*(3), 1743-1756.

Dai, H., Ou, S., Huang, Y., & Huang, H. (2018b). Utilization of pineapple peel for production of nanocellulose and film application. *Cellulose, 25*.

de Andrade, M. R., Nery, T. B., de Santana e Santana, T. I., Leal, I. L., Rodrigues, L. A., de Oliveira Reis, J. H., Druzian, J. I., & Machado, B. A. (2019). Effect of Cellulose Nanocrystals from Different Lignocellulosic Residues to Chitosan/Glycerol Films. *Polymers, 11*(4).

de Melo Fiori, A. P. S., Camani, P. H., dos Santos Rosa, D., & Carastan, D. J. (2019). Combined effects of clay minerals and polyethylene glycol in the mechanical and water barrier properties of carboxymethylcellulose films. *Industrial Crops*

and Products, 140, 111644.

Economics, R. O. o. A. (2022). *Durian: Farming area, Production, and Production per area* www.oae.go.th

Faruk, O., Bledzki, A. K., Fink, H.-P., & Sain, M. (2012). Biocomposites reinforced with natural fibers: 2000–2010. *Progress in Polymer Science, 37*(11), 1552-1596.

Fathi Achachlouei, B., & Zahedi, Y. (2018). Fabrication and characterization of CMC-based nanocomposites reinforced with sodium montmorillonite and TiO2 nanomaterials. *Carbohydrate Polymers, 199*, 415-425.

Feng, X., Meng, X., Zhao, J., Miao, M., Shi, L., Zhang, S., & Fang, J. (2015). Extraction and preparation of cellulose nanocrystals from dealginate kelp residue: structures and morphological characterization. *Cellulose, 22*(3), 1763-1772.

Fitriani, F., Aprilia, S., Arahman, N., Bilad, M. R., Amin, A., Huda, N., & Roslan, J. (2021). Isolation and Characterization of Nanocrystalline Cellulose Isolated from Pineapple Crown Leaf Fiber Agricultural Wastes Using Acid Hydrolysis. *Polymers (Basel), 13*(23).

Fitriani, F., Aprilia, S., Arahman, N., Bilad, M. R., Amin, A., Huda, N., & Roslan, J. (2021). Isolation and Characterization of Nanocrystalline Cellulose Isolated from Pineapple Crown Leaf Fiber Agricultural Wastes Using Acid Hydrolysis. *Polymers, 13*(23).

Fitriani, F., Aprilia, S., Arahman, N., Bilad, M. R., Suhaimi, H., & Huda, N. (2021). Properties of Biocomposite Film Based on Whey Protein Isolate Filled with Nanocrystalline Cellulose from Pineapple Crown Leaf. *Polymers, 13*(24).

Gazonato, E., Alves Domingos Maia, A., Moris, V., & Faulstich de Paiva, J. (2019). Thermomechanical Properties of Corn Starch Based Film Reinforced with Coffee Ground Waste as Renewable Resource. *Materials Research, 22*.

Haafiz, M. K. M., Hassan, A., Zakaria, Z., & Inuwa, I. M. (2014). Isolation and characterization of cellulose nanowhiskers from oil palm biomass microcrystalline cellulose. *Carbohydrate Polymers, 103*, 119-125.

Hidayat, S., Ardiaksa, P., Riveli, N., & Rahayu, I. (2018). Synthesis and characterization

of carboxymethyl cellulose (CMC) from salak-fruit seeds as anode binder for lithium-ion battery. *Journal of Physics: Conference Series, 1080*, 012017.

Jia, F., Liu, H.-j., & Zhang, G.-g. (2016). Preparation of Carboxymethyl Cellulose from Corncob. *Procedia Environmental Sciences, 31*, 98-102.

John, M., & Anandjiwala, R. (2008). Recent developments in chemical modification and characterization of natural fiber-reinforced composites. *Polymer Composites, 29*, 187-207.

Kampeerapappun, P. (2015). Extraction and Characterization of Cellulose Nanocrystals Produced by Acid Hydrolysis from Corn Husk. *Journal of Metals, Materials and Minerals, 25*, 19-26.

Kanikireddy, V., Varaprasad, K., Jayaramudu, T., Karthikeyan, C., & Sadiku, R. (2020). Carboxymethyl cellulose-based materials for infection control and wound healing: A review. *International Journal of Biological Macromolecules, 164*, 963-975.

Khan, A., Jawaid, M., Kian, L. K., Khan, A. A., & Asiri, A. M. (2021). Isolation and Production of Nanocrystalline Cellulose from Conocarpus Fiber. *Polymers, 13*(11).

Khemkaew, S., & Kaewpirom, S. (2016). Effects of Glycerol and PEG-10 dimethicone on Properties of Biofilm

from Durian rind. *The Journal of Industrial Technology (in Thai), 12*(2), 11-21.

Klunklin, W., Jantanasakulwong, K., Phimolsiripol, Y., Leksawasdi, N., Seesuriyachan, P., Chaiyaso, T., Insomphun, C., Phongthai, S., Jantrawut, P., Sommano, S. R., Punyodom, W., Reungsang, A., Ngo, T. M., & Rachtanapun, P. (2021). Synthesis, Characterization, and Application of Carboxymethyl Cellulose from Asparagus Stalk End. *Polymers, 13*(1).

Kulkarni, R. V., Mangond, B. S., Mutalik, S., & Sa, B. (2011). Interpenetrating polymer network microcapsules of gellan gum and egg albumin entrapped with diltiazem–resin complex for controlled release application. *Carbohydrate Polymers, 83*(2), 1001-1007.

Leão, A. L., Cherian, B. M., Narine, S., Souza, S. F., Sain, M., & Thomas, S. (2015). 7 - The use of pineapple leaf fibers (PALFs) as reinforcements in composites. In O.

Faruk & M. Sain (Eds.), *Biofiber Reinforcements in Composite Materials* (pp. 211-235). Woodhead Publishing.

Li, X., Tabil, L. G., & Panigrahi, S. (2007). Chemical Treatments of Natural Fiber for Use in Natural Fiber-Reinforced Composites: A Review. *Journal of Polymers and the Environment, 15*(1), 25-33.

Liu, S., Low, Z.-X., Xie, Z., & Wang, H. (2021). TEMPO-Oxidized Cellulose Nanofibers: A Renewable Nanomaterial for Environmental and Energy Applications. *Advanced Materials Technologies, 6*(7), 2001180.

Lubis, R., Saragih, S., Wirjosentono, B., & Eddyanto, E. (2018). *Characterization of durian rinds fiber (Durio zubinthinus, murr) from North Sumatera* (Vol. 2049).

Ma, H., Zhou, B., Li, H.-S., Li, Y.-Q., & Ou, S.-Y. (2011). Green composite films composed of nanocrystalline cellulose and a cellulose matrix regenerated from functionalized ionic liquid solution. *Carbohydrate Polymers, 84*(1), 383-389.

Mandal, A., & Chakrabarty, D. (2011). Isolation of nanocellulose from waste sugarcane bagasse (SCB) and its characterization. *Carbohydrate Polymers, 86*(3), 1291-1299.

Masrol, S. R., Ibrahim, M. H. I., & Adnan, S. (2015). Chemi-mechanical Pulping of Durian Rinds. *Procedia Manufacturing, 2*, 171-180.

Mendes, C. A. d. C., Ferreira, N. M. S., Furtado, C. R. G., & de Sousa, A. M. F. (2015). Isolation and characterization of nanocrystalline cellulose from corn husk. *Materials Letters, 148*, 26-29.

Meriem, F., Stambouli, H., Gueddira, T., Dahrouch, A., Qaiss, A., & Bouhfid, R. (2016). Extraction and Characterization of Nanocrystalline Cellulose from Doum (Chamaerops humilis) Leaves: A Potential Reinforcing Biomaterial. *Journal of Polymers and the Environment, 24*.

Mohamad Mazlan, M., Kian, L., Fouad, H., Jawaid, M., Karim, Z., & Saba, N. (2022). Synthesis and characterization of carboxymethyl cellulose from pineapple leaf and kenaf core biomass: a comparative study of new raw materials. *Biomass Conversion and Biorefinery*.

Mohammed, A. S. A., Naveed, M., & Jost, N. (2021). Polysaccharides; Classification, Chemical Properties, and Future Perspective Applications in Fields of

Pharmacology and Biological Medicine (A Review of Current Applications and Upcoming Potentialities). *Journal of Polymers and the Environment, 29*(8), 2359-2371.

Mohan, T. P., & Kanny, K. (2015). Thermoforming studies of corn starch-derived biopolymer film filled with nanoclays. *Journal of Plastic Film & Sheeting, 32*(2), 163-188.

Nadeem, H., Athar, M., Dehghani, M., Garnier, G., & Batchelor, W. (2022). Recent advancements, trends, fundamental challenges and opportunities in spray deposited cellulose nanofibril films for packaging applications. *Science of The Total Environment, 836*, 155654.

Nam, S., French, A. D., Condon, B. D., & Concha, M. (2016). Segal crystallinity index revisited by the simulation of X-ray diffraction patterns of cotton cellulose Iβ and cellulose II. *Carbohydrate Polymers, 135*, 1-9.

Ncube, L. K., Ude, A. U., Ogunmuyiwa, E. N., Zulkifli, R., & Beas, I. N. (2020). Environmental Impact of Food Packaging Materials: A Review of Contemporary Development from Conventional Plastics to Polylactic Acid Based Materials. *Materials (Basel), 13*(21).

Nechyporchuk, O., Belgacem, M. N., & Bras, J. (2016). Production of cellulose nanofibrils: A review of recent advances. *Industrial Crops and Products, 93*, 2-25.

Ng, H.-M., Sin, L., Bee, S.-T., Tee, T.-T., & Rahmat, A. (2017). A Review of Nanocellulose Polymer Composites Characteristics and Challenges. *Polymer-Plastics Technology and Engineering, 56*.

Ortega, F., Versino, F., López, O., & García, M. (2021). Biobased composites from agro-industrial wastes and by-products. *Emergent Materials, 5*.

Ouarhim, W., Nadia, Z., Bouhfid, R., & Qaiss, A. (2019). Mechanical performance of natural fibers–based thermosetting composites. In (pp. 43-60).

Oun, A. A., & Rhim, J.-W. (2015). Preparation and characterization of sodium carboxymethyl cellulose/cotton linter cellulose nanofibril composite films. *Carbohydrate Polymers, 127*, 101-109.

Penjumras, P., Rahman, R. B. A., Talib, R. A., & Abdan, K. (2014). Extraction and

Characterization of Cellulose from Durian Rind. *Agriculture and Agricultural Science Procedia, 2*, 237-243.

Pirich, C. L., Picheth, G. F., Machado, J. P. E., Sakakibara, C. N., Martin, A. A., de Freitas, R. A., & Sierakowski, M. R. (2019). Influence of mechanical pretreatment to isolate cellulose nanocrystals by sulfuric acid hydrolysis. *International Journal of Biological Macromolecules, 130*, 622-626.

Prado, K. S., & Spinacé, M. A. S. (2019). Isolation and characterization of cellulose nanocrystals from pineapple crown waste and their potential uses. *International Journal of Biological Macromolecules, 122*, 410-416.

Rachtanapun, P. (2009). Blended films of carboxymethyl cellulose from papaya peel (CMCp) and corn starch. *Nat. Sci.), 43*, 259-266.

Rachtanapun, P., Klunklin, W., Jantrawut, P., Leksawasdi, N., Jantanasakulwong, K., Phimolsiripol, Y., Seesuriyachan, P., Chaiyaso, T., Ruksiriwanich, W., Phongthai, S., Sommano, S. R., Punyodom, W., Reungsang, A., & Ngo, T. M. (2021). Effect of Monochloroacetic Acid on Properties of Carboxymethyl Bacterial Cellulose Powder and Film from Nata de Coco. *Polymers, 13*(4).

Rachtanapun, P., Luangkamin, S., Tanprasert, K., & Suriyatem, R. (2012). Carboxymethyl cellulose film from durian rind. *LWT - Food Science and Technology, 48*(1), 52-58.

Reddy, N., & Yang, Y. (2005). Structure and properties of high quality natural cellulose fibers from cornstalks. *Polymer, 46*(15), 5494-5500.

Rhim, J. W., Wang, L. F., & Hong, S. I. (2013). Preparation and characterization of agar/silver nanoparticles composite films with antimicrobial activity. *Food Hydrocolloids, 33*(2), 327-335.

Romruen, O., Karbowiak, T., Tongdeesoontorn, W., Shiekh, K. A., & Rawdkuen, S. (2022). Extraction and Characterization of Cellulose from Agricultural By-Products of Chiang Rai Province, Thailand. *Polymers (Basel), 14*(9).

Ryu, J. H., Koo Han, N., Lee, J. S., & Jeong, Y. G. (2019). Microstructure, thermal and mechanical properties of composite films based on carboxymethylated nanocellulose and polyacrylamide. *Carbohydrate Polymers, 211*, 84-90.

Santos, R. M. d., Flauzino Neto, W. P., Silvério, H. A., Martins, D. F., Dantas, N. O., &

Pasquini, D. (2013). Cellulose nanocrystals from pineapple leaf, a new approach for the reuse of this agro-waste. *Industrial Crops and Products, 50*, 707-714.

Savadekar, N., & Mhaske, S. (2012). Synthesis of nanocellulose fiber and effect on thermoplastic starch based films. *Carbohydrate Polymers, 89*, 146–151.

Sena Neto, A. R., Araujo, M. A. M., Barboza, R. M. P., Fonseca, A. S., Tonoli, G. H. D., Souza, F. V. D., Mattoso, L. H. C., & Marconcini, J. M. (2015). Comparative study of 12 pineapple leaf fiber varieties for use as mechanical reinforcement in polymer composites. *Industrial Crops and Products, 64*, 68-78.

Shahi, N., Joshi, G., & Min, B. (2020). Effect of Regenerated Cellulose Fibers Derived from Black Oat on Functional Properties of PVA-Based Biocomposite Film. *Processes, 8*(9).

Shankar, S., & Rhim, J.-W. (2016). Preparation of nanocellulose from micro-crystalline cellulose: The effect on the performance and properties of agar-based composite films. *Carbohydrate Polymers, 135*, 18-26.

Shanmugam, K., Ang, S., Maliha, M., Raghuwanshi, V., Varanasi, S., Garnier, G., & Batchelor, W. (2021). High-performance homogenized and spray coated nanofibrillated cellulose-montmorillonite barriers. *Cellulose, 28*(1), 405-416.

Sharma, A., Goswami, S., & Mandal, T. (2018). *Cellulose nanofibers from rice straw: Process development for improved delignification and better crystallinity index*.

Silvério, H., Flauzino Neto, W., Dantas, N., & Pasquini, D. (2013). Extraction and characterization of cellulose nanocrystals from corncob for application as reinforcing agent in nanocomposites. *Industrial Crops and Products, 44*, 427–436.

Su, J., & Zhang, J. (2016). Comparison of rheological, mechanical, electrical properties of HDPE filled with BaTiO3 with different polar surface tension. *Applied Surface Science, 388*, 531-538.

Suhaimi, S. B., Patthrare, I., Saekow, M., & Tongdeesoontorn, W. (2017). Synthesis of methyl cellulose from nang lae pineapple leaves and production of methyl cellulose film. *Current Applied Science and Technology, 17*, 233-244.

Togrul, H., & Arslan, N. (2003). Production of carboxymethyl cellulose from sugar beet pulp cellulose and rheological behavior of carboxymethyl cellulose.

Carbohydrate Polymers, 54, 73-82.

Uetani, K., & Yano, H. (2011). Nanofibrillation of Wood Pulp Using a High-Speed Blender. *Biomacromolecules, 12*(2), 348-353.

Upasen, S., Boonruam, P., Soisuwan, S., Antonio, C., & Wattanachai, P. (2023). Biofilm and Biocomposite Film prepared from Durian Rind and Pineapple Leaf: Synthesis and Characterization. *Engineered Science*.

Vallejo, M., Cordeiro, R., Dias, P. A. N., Moura, C., Henriques, M., Seabra, I. J., Malça, C. M., & Morouço, P. (2021). Recovery and evaluation of cellulose from agroindustrial residues of corn, grape, pomegranate, strawberry-tree fruit and fava. *Bioresources and Bioprocessing, 8*(1), 25.

Xiao, S., Gao, R., Gao, L., & Li, J. (2016). Poly(vinyl alcohol) films reinforced with nanofibrillated cellulose (NFC) isolated from corn husk by high intensity ultrasonication. *Carbohydrate Polymers, 136*, 1027-1034.

Xing, L., Gu, J., Zhang, W., Tu, D., & Hu, C. (2018). Cellulose I and II nanocrystals produced by sulfuric acid hydrolysis of Tetra pak cellulose I. *Carbohydrate Polymers, 192*, 184-192.

Xu, Y., Wu, Z., Li, A., Chen, N., Rao, J., & Zeng, Q. (2024). Nanocellulose Composite Films in Food Packaging Materials: A Review. *Polymers, 16*(3).

Yang, X., Han, F., Xu, C., Jiang, S., Huang, L., Liu, L., & Xia, Z. (2017). Effects of preparation methods on the morphology and properties of nanocellulose (NC) extracted from corn husk. *Industrial Crops and Products, 109*, 241-247.

Yunqing He, X. F., Hui Li. (2019). Carboxymethyl cellulose-based nanocomposites reinforced with montmorillonite and ε-poly-l-lysine for antimicrobial active food packaging. *Applied Polymer, 137*(23), 48782.

Yusmaniar, Y., Julio, E., Rahman, A., Yudanto, S. D., & Susetyo, F. B. (2023). Synthesis of Polyvinyl Alcohol-Chitosan Composite Film using Nanocellulose from Coconut Fibers (Cocos nucifera). *International Journal of Engineering, 36*(11), 1993-2003.

Zarina, S. A., I. (2015). Biodegradable Composite Films based on κ-carrageenan Reinforced by Cellulose Nanocrystal from Kenaf Fibers. *BioResorces, 10*(1), 256-271.

Zhao, G., Lyu, X., Lee, J., Cui, X., & Chen, W.-N. (2019). Biodegradable and transparent cellulose film prepared eco-friendly from durian rind for packaging application. *Food Packaging and Shelf Life, 21*, 100345.

Zhou, L., He, H., Jiang, C., Ma, L., & Yu, P. (2017). Cellulose Nanocrystals from Cotton Stalk for Reinforcement of Poly(Vinyl Alcohol) Composites. *Cellulose Chemistry and Technology, 51*, 109-119.

Zimniewska, M., & Wladyka-Przybylak, M. (2016). Natural Fibers for Composite Applications. In *Fibrous and Textile Materials for Composite Applications* (pp. 171-204).

APPENDICES

APPENDIX A Mechanical properties of films

Table A1 Mechanical properties of CMC_{DH} composite films with different concentrations of nanocellulose (CHNc and PLNc)

Materials	Tensile strength (MPa)	Elongation at break (%)	Toughness (MJ/m^3)
CMC_{DH}-F	1.6 ± 0.2^{a}	$203.3 \pm 8.7^{a,b}$	0.4 ± 0.1^{a}
CMC_{DH}/CHNc(15%)-F	2.8 ± 0.7^{b}	226.5 ± 9.2^{c}	0.6 ± 0.2^{a}
CMC_{DH}/CHNc(30%)-F	3.4 ± 0.4^{b}	221.7 ± 9.1^{c}	$0.8 \pm 0.2^{a,b}$
CMC_{DH}/CHNc(45%)-F	$4.5 \pm 0.8^{c,d}$	197.9 ± 9.9^{a}	1.2 ± 0.3^{b}
CMC_{DH}/PLNc(15%)-F	4.9 ± 0.9^{d}	$214.7 \pm 12.5^{b,c}$	$1.7 \pm 0.6^{c,d}$
CMC_{DH}/PLNc(30%)-F	5.1 ± 1.2^{d}	$216.8 \pm 8.5^{b,c}$	1.9 ± 0.6^{d}
CMC_{DH}/PLNc(45%)-F	$3.8 \pm 0.4^{b,c}$	$214.7 \pm 10.2^{b,c}$	$1.3 \pm 0.2^{b,c}$

Mean ± Standard deviation values within a column in the same group followed by the different letters (a–d) are significantly different ($p < 0.05$)

Table A2 Mechanical properties of CMC_{com} composite films with different concentrations of nanocellulose (CHNc and PLNc)

Materials	Tensile strength (MPa)	Elongation at break (%)	Toughness (MJ/m^3)
CMC_{com}-F	2.3 ± 0.8^{a}	272.6 ± 17.4^{a}	0.9 ± 0.3^{a}
CMC_{com}/CHNc(45%)-F	$2.8 \pm 1.0^{a,b}$	206.9 ± 12.8^{b}	0.7 ± 0.3^{a}
CMC_{com}/PLNc(30%)-F	3.2 ± 0.7^{b}	266.3 ± 13.4^{a}	1.3 ± 0.3^{b}

Mean ± Standard deviation values within a column in the same group followed by the different letters (a–b) are significantly different ($p < 0.05$)

BIOGRAPHY

NAME	MS. Nattapron Siribanluehan
DATE OF BIRTH	4 March 1993
PLACE OF BIRTH	Phra nakhon si ayutthaya
PRESENT ADDRESS	116, Village No. 8, Ban Mai Subdistrict, Phra Nakhon Si Ayutthaya District, Phra Nakhon Si Ayutthaya, 13000
POSITION HELD	Government officer
EDUCATION	Master of Science at the Petroleum and Petrochemical College, Chulalongkorn University Bachelor of Science at King Mongkut's Institute of Technology, Ladkrabang